Report No. BMI-1398

C-25 Metallurgy and Ceramics
(M-3679, 23rd Ed.)

Contract No. W-7405-eng-92

PROGRESS RELATING TO CIVILIAN APPLICATIONS DURING NOVEMBER, 1959

by

Russell W. Dayton
Clyde R. Tipton, Jr.

December 1, 1959

BATTELLE MEMORIAL INSTITUTE
505 King Avenue
Columbus 1, Ohio

DISCLAIMER

TABLE OF CONTENTS

TABLE OF CONTENTS
(Continued)

REPORTS RELATING TO CIVILIAN APPLICATIONS ISSUED DURING NOVEMBER, 1959

BMI-1350 "An Evaluation of the Properties and Behavior of Zirconium-Uranium Alloys", by Arthur A. Bauer.

BMI-1375 "Construction Materials for Various Head-End Processes for the Aqueous Reprocessing of Spent Fuel Elements", by Charles L. Peterson, Paul D. Miller, James D. Jackson, and Frederick W. Fink.

BMI-1380 "Hydrogen Pickup During Corrosion of Zirconium Alloys", by Warren E. Berry, Dale A. Vaughn, and Earl L. White.

BMI-1383 "A Study of the Effects of Fabricating Conditions on Some Properties of Sintered Uranium Monocarbide", by Arch B. Tripler, Jr., M. Jack Snyder, and Winston H. Duckworth.

BMI-1387 "A Visual Study of the Corrosion of Defected Zircaloy-2 Clad Fuel Specimens by Hot Water", by Elmer F. Stephan, Paul D. Miller, and Frederick W. Fink.

BMI-1388 "Effects of Ternary Additions on Aluminum-35 w/o Uranium Alloys", by Norman E. Daniel, Ellis L. Foster, and Ronald F. Dickerson.

BMI-1389 "Survey of End-Capping Methods for Zircaloy-2-Clad Uranium Fuel Elements", by Julius J. Vagi, Roger L. Koppenhofer, and Robert M. Evans.

BMI-1391 "Progress Relating to Civilian Applications During October, 1959", by Russell W. Dayton and Clyde R. Tipton, Jr.

A-1

A. ASSISTANCE TO HAPO

F. R. Shober

A comparison of the creep properties of 15 per cent cold-worked Zircaloy-2 and of annealed Zircaloy-2 is being made. Creep data are being obtained at 290, 345, and 400 C. Tests of 12,000 hr in duration are expected. In studies to develop a fuel-element-leak detector which removes halide fission products from the reactor-coolant streams, experimental work during November included (1) determination of the exchangeability of bromine-82 and AgBr, (2) determination of gross fission-product retention by AgBr columns, and (3) studies to determine possible methods of reducing gross fission-product contamination of AgBr columns.

A thermal-neutron-flux-monitoring system is being developed for the Hanford reactors. Research has continued on the ceramic tube to be used for the flux probe with attention directed to compositional effects on the resistivity of the extruded ceramics. It was found that the resistance of the tubes was a function of the quality of the electrical contact made at the end of the ceramic tube. Hence, the electrical resistivities are being redetermined. In the development of corrosion-resistant welding alloys for use with Hastelloy F, twelve experimental nickel-base alloys have been prepared. Thirteen corrosion specimens of Hastelloy F were welded using filler rods of Hastelloy F and of the 12 experimental alloys. In addition, the 12 experimental alloy-plate specimens were welded with filler of their base composition. Corrosion tests are being initiated.

Mechanical Properties of Zirconium Alloys

L. P. Rice and J. A. VanEcho

Creep and stress-rupture properties of Zircaloy-2 sheet material are being determined in order to provide useful mechanical design data. At present, annealed and cold-worked (15 per cent) Zircaloy sheet is being tested at temperatures of 290, 345, and 400 C in vacuum.

During this report period, two Zircaloy-2 test specimens have ruptured. One was an annealed specimen, and the other was a 15 per cent cold-worked specimen. A brief summary of the available stress-rupture behavior of annealed and cold-worked Zircaloy-2 (excluding the cyclic tests) is presented in Table A-1.

TABLE A-1. STRESS-RUPTURE DATA FOR ANNEALED AND 15 PER CENT COLD-WORKED ZIRCALOY-2 TESTED AT 290, 345, AND 400 C IN VACUUM

Specimen	Condition	Stress, psi	Rupture Time, hr	Elongation, per cent	Minimum Creep Rate, per cent per hr
			290 C (550 F)		
Zr-A-7	Annealed	27,500	0.9	20.3	8.0
Zr-A-6	Annealed	25,000	0.3	44.3	Not measured
7-A-17	Cold worked	37,500	10,883	43.7	0.00006
			345 C (650 F)		
Zr-A-8	Annealed	25,000	858	18.0	0.004
7-1-1	Cold worked	30,000	4,206	12.0	0.00023
			400 C (750 F)		
Zr-A-9	Annealed	21,860	On loading	36.6	--
Zr-A-2	Annealed	21,800	49	21.3	0.15
Zr-A-12	Annealed	17,500	1,036	45.7	0.025
Zr-A-5	Annealed	15,000	3,664	46.0	0.006

Tests have been started on two additional annealed specimens of Zircaloy-2 (Zr-A-27 at 290 C under a stress of 12,500 psi and Zr-A-26 at 400 C at a stress of 9,000 psi). At the present time there are 20 tests in progress.

Development of a Fuel-Element Leak Detector

J. E. Howes, Jr., T. S. Elleman, and D. N. Sunderman

The purpose of the program is to investigate the feasibility of using AgX columns to selectively remove halide fission products from reactor-coolant streams. Progress during this work period on the program has included (1) determination of the exchangeability of bromine-82 and AgBr, (2) determination of gross fission-product retention by AgBr columns, and (3) studies to determine possible methods of reducing gross fission-product contamination of AgBr columns.

The extent of exchange between bromine-82 and AgBr at 75 and 180 F was determined by passing bromine-82 solution through 16 to 50-mesh AgBr columns at flow rates of 0.2, 0.5, 1.0, and 1.5 gal per min. Experiments carried out at 180 F gave bromide-retention values ranging from 13 to 20 per cent, while retention values at 75 F ranged from 36 to 45 per cent. The bromine-82 was washed off the column at a rate of 50 per cent of the retained bromine-82 per min at 180 F, so complete isotopic equilibrium on the column was reached in approximately 5 min.

A-3

Gross fission-product contamination of AgBr columns was determined as a function of flow rate and column size. One-inch-high by 1-in.-diameter and 2-in.-high by 1-in.-diameter columns retained from 2.5 to 4.8 per cent of the fission products at flow rates from 0.2 to 1.5 gal per min. Decontamination factors (per cent iodine-131 retained divided by per cent fission products retained) ranged from 10 to 26. The gross fission products were not rapidly washed from the columns so the equilibrium concentration of fission products on the column would appear to be quite high.

Since the sensitivity of the leak-detection system will depend on the selective retention of only halide fission products, an effort is being made to develop a method of reducing gross fission-product retention on the AgBr columns. In initial experiments, fission-product solution was passed through columns of silica gel and glass wool prior to passing through the AgBr column. It was anticipated that the majority of the fission-product activity would be adsorbed and filtered out before entering the AgBr column. However, neither the silica gel nor the glass wool retained sufficient fission-product activity to reduce contamination of the AgBr exchange columns.

Experiments are now under way in which fission-product solution will be passed through a column of a complexing agent, such as EDTA, before passing through the AgBr column. The formation of soluble fission product-EDTA complexes should keep the fission products in solution and not permit the adsorption on the AgBr column.

Thermal-Neutron-Flux Monitoring System

J. W. Lennon, D. R. Grieser, P. M. Steinback,
and W. H. Goldthwaite

A thermal-neutron-flux measuring instrument previously developed (see BMI-1083) is serving as the basis for the development of a thermal-neutron-flux monitoring probe with extended life and increased range for Hanford reactors. In the flux-monitoring device, thermal neutrons cause fission of uranium-235 in a $MoSi_2$-Al_2O_3-UO_2 ceramic tube. Another similar ceramic tube, containing depleted uranium rather than enriched uranium, is electrically heated to the same temperature. The electric power then can be directly correlated with thermal-neutron flux.

Research was continued on the ceramic tubes for the flux probe. Attention was directed to compositional effects on resistivity of the extruded ceramic. Recent improvements in applying contacts to the ends of the ceramic tubes have revealed that the measured resistance is a critical function of the quality of the contact. Poor contacts in some cases were found to have a resistance 10 to 20 times the resistance of the element. Consequently, most of the previous determinations of element resistance as a function of $MoSi_2$ content have been invalidated. It was previously indicated that compositions containing 47 to 49 w/o $MoSi_2$ possessed the desired resistance, whereas the recent work indicates that the composition range with the most favorable resistance values lies somewhat below 47 w/o $MoSi_2$. An accurate redetermination of the resistance of lower $MoSi_2$ compositions is to be made early in December. An electropotential method of measurement will allow the actual element resistances to be determined independently of any variation in the resistance of the current-carrying contacts. The contact behavior can

then be evaluated through comparing the resistance measured by the electropotential method to that determined from the voltage drop and current through the end contacts. It will then be possible to study the stability of the element and contact resistances separately. Attempts to use an equipotential measuring technique were defeated previously by extremely high contact resistance.

The present contact attachment technique employs the geometry described in BMI-1391: that of a wire or sleeve brazed to the circumference at each end of the ceramic tube. Trial contacts have been made using stainless steel, Kovar, molybdenum, platinum, and tantalum as the contact metal. Nicrobraz Standard braze was found to wet both the ceramic and these metals. It was also revealed that the amount of braze must be closely controlled to avoid brittleness or excessive alloying.

In another study this month, it was established that ceramic tubes containing 93 per cent enriched UO_2 powder, fabricated in the same manner as those containing depleted UO_2 powder, showed pertinent properties similar to those containing depleted UO_2.

Purchasing and fabrication of some of the probe components have begun.

In the coming month, the most desirable of the ceramic-tube compositions and contact metals will be selected on the basis of the detailed evaluations of stability and favorable electrical resistance. Elements will then be produced in quantity, and the most satisfactory of the lot will be selected for the construction of probes. One pair of these tubes will be placed in a full-size thermal mock-up of the prototype probe, and operated under simulated-service conditions, using two electrically heated ceramic tubes rather than employing fission power. This will be done in order to study the parameters influencing the thermal behavior of a complete unit.

Consideration of design parameters will continue, using information provided from the thermal mock-up tests and leading to the fabrication of the first prototype probes.

Development of Corrosion-Resistant Welding Alloys for Use With Hastelloy F to Contain Decladding Solutions

M. E. Langston, R. E. Monroe, C. L. Peterson, and W. K. Boyd

The objective of this program is to develop corrosion-resistant welding alloys for use with vacuum-melted low-carbon Hastelloy F employed as a container material for spent fuel-element decladding solutions. Twelve nickel-base alloys will be prepared and evaluated in the current phase of the work.

Solution-annealed strip material of all 12 experimental nickel-base alloys has been prepared. Information was obtained on the chemical composition of a few selected alloys and the hardness and microstructure of all experimental nickel-base alloys in the solution-annealed condition.

The data in Table A-2 indicate that the actual compositions are generally in good agreement with the intended values. Exceptions are the high copper content in Alloy 6 and the high manganese contents and the low silicon contents in Alloys 6 and 11.

A-5

Variations in manganese and silicon within the ranges shown for the three alloys are expected to have little or no significant effect on welding behavior and corrosion resistance. On the other hand, the high copper content in Alloy 6 is of importance in respect to these two properties, and for this reason another copper determination will be made. Additional carbon analyses, as well as nitrogen determinations, will be made to aid in the identification of minor phases in the alloys.

TABLE A-2. CHEMICAL COMPOSITIONS OF THREE EXPERIMENTAL NICKEL-BASE ALLOYS[a]

	Chemical Composition, w/o									
Alloy	C	Ni	Cr	Mo	Cu	Nb	Ti	Mn	Si	Fe
2	0.02	45.0	22.0	6.0	2.0	2.0	--	0.60	0.40	22.0
	(0.01)	ND	(22.0)	(5.6)	(1.6)	(1.95)	--	(0.70)	(0.44)	ND
6	0.02	45.0	22.0	3.0	2.0	--	1.0	0.60	0.40	26.0
	(0.01)	ND	(22.2)	(3.3)	(2.8)	--	(1.2)	(0.85)	(0.21)	ND
11	0.02	45.0	22.0	6.0	2.0	--	1.0	0.60	0.40	23.0
	(0.01)	ND	(22.2)	(6.4)	(1.8)	--	(1.2)	(0.76)	(0.19)	ND

(a) Parentheses indicate actual analyses, all others intended values. ND indicates that no analysis was made.

Hardness data for the solution-annealed materials are given in Table A-3. In general, the hardness values of the annealed materials fell within the range previously established for the alloys. Although a direct comparison of hardness and composition is somewhat complicated by the fact that three different annealing temperatures were used, a few general observations can be made. For example, increasing molybdenum from 3 to 9 w/o resulted in a higher hardness in the annealed material; whereas, copper did not appear to affect hardness.

Metallographic examination of the annealed materials revealed a generally fine-grained matrix with randomly dispersed minor phases. The amount and appearance of these secondary phases were dependent on alloy composition. In general, less second phase was noted in the titanium-bearing alloys than in those containing niobium. An increase in molybdenum content from 3 to 9 w/o appeared to result in an increase in the amount of second phase after annealing. Variations in copper from 1 to 3 w/o had no noticeable effect on microstructure. Studies on the identity of the minor phases in the annealed structures will be continued.

The welding of specimens for corrosion studies was completed. Thirteen specimens of Hastelloy F and 12 specimens of the experimental alloys were prepared. One of the Hastelloy F specimens was welded with Hastelloy F filler, while the remaining specimens were welded using one of each of the 12 experimental alloys as the filler material. In addition, the 12 experimental alloy plate specimens were welded with filler of their base composition.

TABLE A-3. HARDNESS OF EXPERIMENTAL NICKEL-BASE-ALLOY STRIP MATERIAL

Solution Annealed for 1 Hr at 1950 to 2150 F and Water Quenched

Alloy	Nominal Addition[a], w/o				Solution Annealing Temperature, F	Rockwell B Hardness
	Mo	Cu	Nb	Ti		
1	6	1	2	--	2150	81.5
2	6	2	2	--	2150	81.5
3	6	--	--	0.5	2050	80.0
4	6	--	--	1.0	2050	78.5
5	3	2	--	0.5	1950	76.0
6	3	2	--	1.0	1950	74.0
7	6	3	2	--	2150	82.0
8	9	1	2	--	2150	87.0
9	3	1	2	--	2050	84.0
10	6	2	--	--	2050	78.0
11	6	2	--	1	2050	77.0
12	3	2	2	--	2050	77.5

(a) Base composition: iron-45 w/o nickel-22 w/o chromium-0.6 w/o manganese-0.45 w/o silicon-0.02 w/o (maximum) carbon.

Welding was done by the inert-gas-shielded tungsten-arc process, using sheared sheet as filler material. Argon gas was used for shielding. The weld specimens were beveled to give a single V joint and were clamped for welding. Welds were made with a single pass and an argon gas backup. The tungsten electrode operated on negative polarity.

Radiographic and metallographic examinations of the welded specimens showed the welds to be of good quality.

The experimental alloys containing titanium gave welds that were somewhat dirty in appearance. Otherwise, all alloys performed satisfactorily as filler material.

The exposure of unwelded coupon-type specimens of Hastelloy F and all 12 experimental alloys to boiling Sulfex solutions has been started. Exposure of Hastelloy F and Alloys 1 to 6 to boiling Niflex solution also is under way. Coupons are being exposed both to the vapor and to the liquid phases for five 24-hr periods. At present, there are not sufficient data to indicate trends. Good reproducibility of the corrosion rates for duplicate specimens has been obtained.

Coupon-type specimens are being machined from the welded stock and will be exposed upon completion of the exposure of the unwelded coupons.

B-1

B. DEVELOPMENTS FOR ALUMINUM-CLAD FUEL ELEMENTS

R. J. Carlson and N. E. Daniel

Aluminum-35 w/o uranium alloys containing small additions of tin or zirconium are being evaluated on the bases of casting and fabricating characteristics, mechanical properties, and corrosion resistance in 200 C water. The room-temperature hardnesses of alloys containing up to 3 w/o of these ternary additions were all within a range of 10 DPH, i.e., between 58 and 68 DPH. Heat treatment of the alloys at 600 C for periods up to 48 hr revealed that the peritectic reaction proceeded at a higher rate in the alloys containing tin than it did in similar alloys containing zirconium.

Preparation of Aluminum-Uranium Alloys

N. E. Daniel, E. L. Foster, and R. F. Dickerson

In order to investigate the effects of tin and zirconium additions upon the casting and fabricating characteristics and upon the physical properties of an aluminum-uranium alloy, alloys of 35 w/o uranium containing up to 3 w/o tin or zirconium have been prepared and are being evaluated.

The metallographic examination of the alloys in both the as-cast and extruded conditions and after heat treatments at 600 C for periods of 8, 24, and 48 hr have been completed. In all the specimens examined, it was noted that the eutectic portion had spheroidized after 24 hr at temperature. The examinations also revealed that the UAl_3-UAl_4 reaction had progressed at a higher rate in the alloys containing tin than it did in alloys containing equal quantities of zirconium. In all cases the reaction proceeded more rapidly in those alloys containing the smaller ternary additions.

Hot-hardness determinations have been made on all of the extruded alloys at temperatures up to 600 C. The room-temperature hardnesses of all materials were within the range of 58 to 68 DPH, and this spread, expressed in terms of per cent, did not change appreciably up to 300 C. However, plots of the data on semilog paper illustrated that a greater rate of decrease in hardness with temperature occurred in all alloys at temperatures above 300 to 350 C.

Corrosion tests are being conducted in 200 C demineralized water. From the results obtained after 20 days of exposure there are indications that vacuum-melted alloys containing zirconium are less susceptible to attack than air-melted binary alloys of aluminum-35 w/o uranium or air-melted materials containing either tin or zirconium. The weight gains exhibited by the air-melted material are two to three times those exhibited by the vacuum-melted alloys containing zirconium.

B-2

Casting studies preparatory to making enriched castings of the alloys in the form of hollow cylindrical extrusion billets have been initiated. Steel molds with hollow steel cores are being used. In an effort to produce sound, nonporous ingots containing zirconium by air-melting techniques, master alloys of the approximate composition of $ZrAl_3$ were prepared under a dynamic vacuum. The master alloy was introduced into the molten aluminum in the form of 1/4-in. or smaller particles. These melts made with the $ZrAl_3$ master alloy and melts made with virgin tin are being evaluated by chemical analyses and radiographic examinations. It is planned to ship six of these full-size extrusion billets to another site for fabrication studies.

Future work will be concerned with the tensile testing of extruded materials at elevated temperatures and with the continuation of the corrosion tests now in progress. Upon completion of the tensile testing, stress-rupture and creep data will be obtained on selected alloy compositions. Further casting studies are also contemplated before the billets containing enriched uranium are made.

C-1

C. RADIOISOTOPE AND RADIATION APPLICATIONS

D. N. Sunderman

A continuing program in under way for the Office of Isotopes Development in the fields of radioisotope application and radiation chemistry. Studies include the development of radiotracer applications in quality control, intrinsic tracers for process control, structural effects in radiation-induced graft polymerization, and the nitration of hydrocarbons.

The application of neutron-activation analysis to the determination of macro constituents in portland cement appears qualitative at best. Errors of 10 per cent arise from thermal-flux variations, radioassay statistics, and nuclear reactions other than those which produce the desired radionuclide. This specific application is not competitive with other instrumental techniques and further work is not planned.

Radiometric titrations for the determination of aluminum and iron in the same solution appear very promising. Preliminary results indicate an accuracy of better than ±2 per cent for each element. EDTA is the titrant and the radioactive salts $Ag^{110}IO_3$ and $Y_2^{91}(C_2O_4)_3$ are indicators for the aluminum and iron endpoints, respectively.

The investigation of radioisotopes of other elements as substitutes for iron-59 in the intrinsic-tracer iron-removal study indicates that other elements may be used in similar studies but are not useful as substitutes for iron. The purpose of this evaluation was to find a tracer less prominent in biological processes. The effect of salt concentrations upon radioassay efficiency in the dip-counting system has been evaluated. Experimental results support early theoretical calculations by indicating that no problem will exist.

The effect of radiation dose upon number of grafting sites has been evaluated in the range of 1.7×10^5 to 1.3×10^7 rep. This study will be carried to 10^8 rep. The number of active sites per monomer unit resulting from a radiation dose of 5.6×10^5 rep was determined for a variety of methacrylates. Results indicate that branched-chain polymers develop a larger number of such sites than do the straight-chain species.

A variety of radiation and thermal nitration experiments have been completed and the results of chemical analyses are reported. Liquid-phase nitration seems to favor the production of nitrocyclohexane. Results also show that nitration is promoted by radiation for reaction times less than about 20 hr, while other effects predominate for longer reaction times. This effect will be studied in more detail.

C-2

Development of Radioactive-Tracer Quality-Control Systems

C. W. Townley, C. T. Brown, R. Lieberman,
and D. N. Sunderman

Activation analyses have been performed on the following samples: aluminum metal, iron metal, magnesium nitrate, manganese sulfate, silicon dioxide, and sodium nitrate. These samples were investigated in order to determine what corrections, if any, must be made to account for the following fast-neutron reactions: $Fe^{56}(n,p)Mn^{56}$, $Mg^{24}(n,p)Na^{24}$, $Si^{28}(n,p)Al^{28}$, and $Al^{27}(n,p)Mg^{27}$. Since each of these elements is present in cement and cement raw materials, the fast-neutron reactions would yield high results for manganese and sodium, and high or low results for aluminum; the latter depending on the relative magnitude of the $Si^{28}(n,p)Al^{28}$ and $Al^{27}(n,p)Mg^{27}$ reactions. It has already been determined that the $Al^{27}(n,\alpha)Na^{24}$ reaction will yield results 0.1 per cent low in aluminum and correspondingly 0.1 per cent high in sodium. Table C-1 is a summary of the results obtained for each of the fast-neutron reactions.

TABLE C-1. THE EFFECT OF FAST-NEUTRON REACTIONS ON THE ACTIVATION ANALYSIS OF CEMENT AND CEMENT RAW MATERIALS

Fast-Neutron Reaction	Effect	Apparent Magnesium Product per Magnesium Target Material[a]	Error in a Typical Cement Sample[b], per cent
$Al^{27}(n,\alpha)Na^{24}$	Low Al, high Na	0.001	-0.15 in Al_2O_3 +3.57 in Na_2O
$Al^{27}(n,p)Mg^{27}$	Low Al	0.010	-1.27 in Al_2O_3
$Si^{28}(n,p)Al^{28}$	High Al	0.005	+2.07 in Al_2O_3
$Mg^{24}(n,p)Na^{24}$	High Na	No trace of Na^{24} activity	None
$Fe^{56}(n,p)Mn^{56}$	High Mn	0.0004	+2.00 in Mn_2O_3

(a) The composition of product and target material is expressed as the oxide, i.e., Na_2O, MgO, Al_2O_3, Fe_2O_3, Mn_2O_3, and SiO_2.

(b) NBS standard sample No. 177. Net result for Al_2O_3 is +0.65 per cent.

The contribution of the fast-neutron reactions is not negligible. However, the accuracy in the results for the most part has not been better than ±10 per cent. The poor results must, therefore, be a combination of several variables, not the least of which is accurate flux measurement. It must be assumed that the present application of activation analysis is a semiquantitative method, but results to ±1 per cent are not probable.

The development of a radiometric method of determining aluminum and iron in portland cement has continued during this report period. An EDTA titration procedure employing $Ag^{110}IO_3$ as an endpoint indicator for the aluminum titration and $Y_2^{91}(C_2O_4)_3$ as an indicator in the iron titration is being studied.

The conditions have been investigated for titrating iron using a solution 40 to 50 ml in volume containing 11.2 mg of Fe(III). Titrations have been performed with pH values ranging from 4 to 8. At pH 4 the yttrium has not complexed with the EDTA, so no endpoint has been obtained at this pH. No endpoint was obtained at pH values of 7 and 8 because of hydrolysis of the iron-EDTA complex. At pH 6 the accuracy of the method

was no better than 20 per cent. Possibly some hydrolysis occurred even at this pH. At pH 5 the titration has worked well, with the error ranging from 0.2 to 3 per cent.

Both a sodium hydroxide-boric acid buffer and an ammonium acetate buffer have been employed in the iron titration. The results have been slightly better with the sodium hydroxide-boric acid system. Tartaric acid has been added to the iron solution before increasing the pH in order to prevent the precipitation of ferric hydroxide.

The study of the aluminum titration has continued with the use of a 40 to 50-ml solution containing 11.3 mg of Al(III). At a pH of 8 the titration has been performed successfully with errors of less than 2 per cent. A sodium hydroxide-boric acid buffer has been used, and tartaric acid has been added to prevent precipitation of aluminum hydroxide. At pH 8 heating has been found to be unnecessary to achieve satisfactory results. Sodium hydroxide is used to neutralize the solution before addition of the buffer, since ammonium hydroxide was found to be undesirable. The ammonia complexed the silver and dissolved the $Ag^{110}IO_3$ before the endpoint of the titration was reached.

One attempt was made to determine the iron and aluminum consecutively in the same solution. A solution of aluminum and iron containing tartaric acid and buffered at pH 5 was titrated with standard EDTA in the presence of $Y^{91}(C_2O_4)_3$. The iron endpoint was determined with an accuracy of 0.2 per cent. The pH was raised to 8 with sodium hydroxide, more buffer was added, and $Ag^{110}IO_3$ was added. The titration was continued to complex all of the yttrium remaining, and the aluminum was titrated. The aluminum endpoint was determined with an accuracy of 1.7 per cent.

During the next report period the development of the radiometric method of analysis for aluminum and iron will be completed. The experimental conditions will be varied in an attempt to reduce the error in the aluminum titration, and a limit of precision and accuracy will be placed on the method.

Use of Intrinsic Radioactive Tracers for Process Control

J. L. McFarling, J. F. Kircher, and D. N. Sunderman

During November, work on this program has continued along the lines indicated in BMI-1391.

Experiments on iron precipitation with ammonia have been carried out using radiotracers other than iron-59. Radioactive antimony, chromium, copper, manganese, and zinc were tested in these experiments. The results indicate that some of the radiotracers tested could be used for an independent indication of solution pH; however, none of those tested would give an accurate and reliable measurement of the iron concentration in solution. At present it does not appear likely that a substitute for iron-59 will be found which closely approximates the iron behavior in this process. Further experiments along these lines are not planned at this time.

C-4

Experiments have been initiated to ascertain the effects of various salt concentrations on the observed counting rate of the dip counter. Preliminary results indicate that these effects are very small or nonexistent. Additional tests are being made, and complete results will be reported next month.

The design of an operating model of an iron-removal process is nearly complete. This model will be used for studying various radiotracer iron-removal application problems under closely simulated process conditions.

A paper evaluation of iron-removal applications in all types of nonferrous-metals refining is now under way. The object of this study is to pinpoint likely radiotracer applications, which can then be demonstrated in the small-scale process equipment to be constructed.

Next month's work will include confirmation of the preliminary experimental results reported here and in BMI-1391. The evaluation of other iron-removal applications will be continued. The process-model design study will be completed, and procurement and construction of the necessary equipment will be initiated during the coming month.

Graft-Polymerization Studies

I. S. Ungar, J. F. Kircher, W. B. Gager,
and R. I. Leininger

During this month the investigation of radiation-induced free radicals and grafting of polymethacrylates was continued. The EPR spectra of polymethylmethacrylate (PMMA) was further investigated. A sample of the polymer was irradiated in a vacuum, and its EPR spectrum was measured. A small amount of methylmethacrylate (MMA) was added, and the spectrum was determined once more. Unlike the sample in which MMA was added before irradiation, this spectrum became broad and less resolved, instead of narrow and more resolved. This seems to indicate that the spectrum observed in commercial PMMA and laboratory-prepared PMMA contaminated with monomer is not due to a reaction of monomer with irradiated polymer. Monomer must be present during the irradiation for the highly resolved spectrum to appear. The effect of temperature on the spectrum of irradiated PMMA was studied. Pure polymer was irradiated in a vacuum and its EPR spectrum determined. The sample was then slowly heated in the spectrometer cavity. As the temperature increased from 24 to 50 C the number of active sites decreased, with no change in spectrum shape or resolution.

A study of the effect of total dose on site formation was begun. The results obtained are in Table C-2. A plot of dose versus sites per monomer unit on log-log paper results in a straight line. A sixth sample is being irradiated to a dose close to 10^8 rep to determine if the number of sites still falls on the same line or is dropping off. A comparison of the spectra at increasing dose shows a gradual change in shape. At doses below 3.4×10^5 rep only a single line is present. As the dose increases more lines appear until at a dose of 6.1×10^6 rep and higher the spectrum resembles that of irradiated commercial PMMA or pure PMMA contaminated with monomer. It is known

that radiation-induced chain scission in methacrylates may produce small fragments and even monomer. These fragments in the polymer give rise to the same spectrum as that formed by the addition of monomer to polymer before irradiation.

TABLE C-2. EFFECT OF TOTAL DOSE ON SITE FORMATION IN PMMA

Sample	Dose, rep	Sites per Monomer Unit
1	1.7×10^5	3.1×10^{-4}
2	3.4×10^5	4.9×10^{-4}
3	1.4×10^6	1.3×10^{-3}
4	6.1×10^6	3.9×10^{-3}
5	1.3×10^7	6.0×10^{-3}

Additional EPR spectra were obtained on other methacrylates. Tentative values for number of sites per monomer unit are given in Table C-3. The value for polyethylmethacrylate seems high with respect to the others and will be checked. All the polymers used in this study were produced by radiation polymerization and subsequent reprecipitation. The number of sites listed are a result of a dose of 5.6×10^5 rep. It may be seen that branching increases the number of sites over that of the straight-chained polymer. All of the above polymers have been grafted with vinylpyrrolidone. The results of this experiment will be available in the next report.

TABLE C-3. SITE FORMATION IN METHACRYLATES GIVEN DOSE OF 5.6×10^5 REP

Polymer	Sites per Monomer Unit
Polyethylmethacrylate	3.5×10^{-3}
Polypropylmethacrylate	3.8×10^{-4}
Polyisopropylmethacrylate	6.0×10^{-4}
Polybutylmethacrylate	3.9×10^{-4}
Poly-tert-butylmethacrylate	1.6×10^{-3}
Polycyclohexylmethacrylate	3.6×10^{-4}

Next month the study of radiation-produced free radicals in methacrylates will be continued. An investigation of total dose as a function of site production will be made for other methacrylates, and site production will be measured by the chemical method for comparison with the values obtained from EPR spectroscopy.

Nitration of Hydrocarbons

M. J. Oestmann, G. A. Lutz, E. J. Kahler,
and J. F. Kircher

During November, twelve irradiation and thermal runs were completed with the cyclohexane-nitric acid system. Analytical results have been obtained for about half of these runs as well as for runs made during October. All results are reported in Table C-4.

TABLE C-4. PRODUCT ANALYSES FOR NITRIC ACID-CYCLOHEXANE RUNS[a]

Run	Temperature, C	Time, hr	Gamma Dose, 10^6 rads	Product Analysis[b], w/o of recovered organic solution						Adipic Acid or Other Solids, g
				$C_6H_{11}NO_2$	$(C_6H_{11})_m(NO_2)_n$	$C_6H_{11}ONO_2$	$(C_6H_{11})_2$	$C_6H_{11}OH$	$C_5H_{10}C=O$	
24	60	20	3.8	0.96	0.04	--	0.07	--	Trace	0.90
25	60	20	--	0.21	Trace	--	Trace	--	--	<0.01
26	60	65	12	2.3	0.06	--	0.12	Trace	Trace	0.75
27	60	65	--	3.5	0.16	0.04	0.12	Trace	Trace	2.35
12	60	117	17	1.1	0.12	--	0.09	0.05	0.03	0.6
10	60	117	--	3.0	0.14	--	0.04	Trace	Trace	2.8
15	110	20	3.8	4.5	Trace	Trace	0.21	0.32	0.04	0.85
13	110	20	--	4.2	--	--	0.11	0.15	0.07	1.1
16	110	20	--	4.3	Trace	0.07	0.4	0.3	0.04	1.13
17	110	20	3.8	3.0	--	Trace	--	--	--	0.069
18	110	20	--	2.8	--	0.05	--	Trace	Trace	0.022
19	140	20	3.8	7.3	--	Trace	0.13	0.5	0.2	0.4
22	140	20	3.8	3.6	--	--	--	Trace	Trace	0.095

(a) All runs made at 10/1 mole ratio of cyclohexane/nitric acid in glass vessels.

(b) Does not include solid products.

C-7 and C-8

In all runs, the mole ratio of cyclohexane to nitric acid was 10/1. Reactions were carried out in a glass vessel over a temperature range from 60 to 140 C. Samples were irradiated from 20 to 117 hr, corresponding to absorbed doses of 3.8×10^6 to 1.7×10^7 rads. In the thermal runs, the system was heated but not irradiated.

The six liquid products, previously identified, are nitrocyclohexanes, a polynitro compound, cyclohexyl nitrate, dicyclohexyl, cyclohexanol, and cyclohexanone. Adipic acid has been identified in the solid-product mixture. Gas chromatography and infrared techniques are used to analyze the products. In all runs, the nitrocyclohexane was produced in much larger quantities than the other products.

To study the effect of phase on the nitration reaction, Runs 15 and 16 were made at 110 C in the liquid state and 17 and 18 in the vapor state. Irradiation Runs 19 and 22 were made at 140 C in the liquid and vapor states, respectively. Identical temperatures, reaction times, and charge compositions were used in each pair of runs. At both 110 and 140 C, the amount of nitrocyclohexane formed is larger in the liquid phase than in the vapor phase.

Severe oxidation occurred when liquid-phase runs were attempted at 140 C. For this reason the maximum temperature in future runs will be limited to about 140 C.

The results show that the nitration reaction is promoted by radiation when the reaction time is short (~20 hr). However, for longer reaction times, it appears that radiation reduces the amount of nitration. More runs are needed to confirm this effect of radiation. This effect will be investigated further by carrying out runs for less than 20 hr.

Future work will include studies of the effect of nitric acid concentration, and possibly other nitrating agents, and chain-transfer agents.

D-1 and D-2

D. VARIABLE-MODERATOR REACTOR CRITICAL-ASSEMBLY STUDIES

R. A. Egen, L. Bettenhausen, W. S. Hogan,
D. A. Dingee, and J. W. Chastain

Critical-assembly research will be performed by Battelle to support the development of the Variable-Moderator Reactor. This reactor concept is being studied by the Advanced Technology Laboratories (ATL) of American-Standard Corporation. The fuel for this reactor consists of slightly enriched VO_2 pellets placed in aluminum tubes about 0.5 in. in diameter and 62 in. long. The active fuel length is 48 in., starting 6 in. from the bottom of the tube. The pins are arranged in hexagonal arrays of 37 or 61 inside a hexagonal can or shroud which separates coolant water from moderator water. Since the program is designed to check calculational procedures to be used on the VMR and is not an engineering mock-up, the experiments will be run near atmospheric conditions. Variations in void conditions in the coolant will be simulated by liquids with lower hydrogen densities at room temperature than water. Design of the assembly, a joint effort of ATL and Battelle, has been completed for all major components, including the reactor base plate, stand, and core vessel, and materials and equipment have been ordered. Samples of the liquids which will be used to simulate boiling water, furfuryl alcohol, and furfural, have been received, and experiments to evaluate compatibility and decomposition are under way.

In writing the Hazards Summary Report and Fuel-Handling Manual, a preliminary experimental program has been outlined. Four values of pin pitch, three of fuel-element pitch, and four void fractions will be investigated. Except for one case, the core will consist of 37 fuel elements with 61 fuel pins per element. In one case the core will contain 61 fuel elements with 37 pins per element.

It is expected that during the next month the Hazards Summary Report and Fuel Handling Manual will be completed. The reactor stand and associated equipment (core vessel, base plate, plumbing, etc.) will be in the construction phase.

F-1

F. RESEARCH FOR AEC REACTOR DEVELOPMENT DIVISION PROGRAM

S. J. Paprocki and R. F. Dickerson

REACTOR MATERIALS AND COMPONENTS

R. F. Dickerson

The studies concerned with stabilizing UO_2 by additions of La_2O_3 or Y_2O_3 plus CaC have been continued. Materials which are stable in air at 1760 C have been produced. Further study indicates that a further reduction in thermal-neutron absorption cross section may be effected by the substitution of MgO for the CaO addition. The pressure calibration of the die being used in connection with the high-temperature high-pressure solid-state studies has been accomplished to 120,000 atm. Previous work at normal pressures has shown that Sc_2O_3 does not react with UO_2; however, samples of UO_2 and Sc_2O_3 subjected to various pressures at temperatures above 1000 C have shown limited reaction to form a small amount of solid solution.

Eight capsules containing Type 347 stainless steel impact, fatigue, and tensile specimens have been irradiated in the ETR at ambient reactor-coolant temperatures since June, 1958, and three additional capsules have been irradiated since August, 1959. Exposures up to 4.3×10^{21} nvt have been obtained to date. At the present time no data on the effects of irradiation on mechanical properties in Type 347 stainless are available for exposures greater than 3.76×10^{21} nvt.

Because of difficulties encountered in cold rolling niobium-base binary alloys of 1.83 w/o chromium and 4.33 w/o zirconium and several niobium-base ternary alloys, an attempt was made to warm roll the forged billets at 800 F. The results were excellent, and reductions of about 70 per cent were obtained. Final reduction was successfully accomplished by cold rolling with intermediate anneals. The results of studies concerned with the development of water-corrosion-resistant niobium alloys indicate that additions of titanium, vanadium, or zirconium give marked improvement. The most corrosion-resistant alloys are those containing 45 a/o zirconium or ternary additions of 28 a/o titanium-6 a/o chromium. Screening tests are in progress with alloys containing additions of cerium, palladium, and yttrium.

The testing device or capsule being designed for the in-pile creep of Zircaloy-2 will provide a specimen temperature of 650 F during test. Additional internal-friction data substantiate earlier information which indicated that strain aging could occur in Zircaloy-2. In addition, the electron-transmission studies of thin films of zirconium and Zircaloy-2 are being continued, and strain-aging studies by tensile tests are in progress.

Since there is a possibility that the oxygen content of sodium may affect the optical properties of its reflecting surfaces, the technique of ellipsometry is being investigated as a possible means of determining oxygen concentrations below the 10-ppm level. Other techniques being considered for this analysis are electrical-resistivity measurements, polarographic studies, and mass spectrographic analyses.

F-2

Valence Effects of Oxide Additions to Uranium Dioxide

W. B. Wilson, A. F. Gerds, and C. M. Schwartz

An investigation is being conducted on the stabilizing influence of oxide additions to uranium oxide. Previously prepared specimens, containing suitable additions to La_2O_3 or Y_2O_3, and La_2O_3 or Y_2O_3 plus CaO, have proved to be stable in air at 1760 C. These specimens had been sintered in vacuum. Specimens presently are being made by adding La_2O_3 to U_3O_8 and sintering in air at 1200 C. Specimens containing 40, 50, and 60 mole per cent additions of La_2O_3 were found to be colored dark blue, dark red, and orange red respectively. The compacts were crushed and resintered at 1200 C. Portions of each will be heated in air at higher temperatures to determine their stabilities. In addition, they will be analyzed chemically and by X-ray diffraction, subsequent to the evaluation of their electrical characteristics.

A further reduction of cross section appears feasible by substitution of MgO for CaO in the ternary oxide compacts. To evaluate this hypothesis, a compact containing UO_2-25 mole per cent Y_2O_3-25 mole per cent MgO is being prepared. After crushing and sintering a second time, this compact also will be analyzed.

High-Pressure High-Temperature Solid-State Studies

W. B. Wilson and C. M. Schwartz

An investigation is being conducted to determine the effects of high pressure and high temperature on the uranium-oxygen system and on reaction of uranium oxide with various mixed oxides.

Additional work was performed to extend the pressure calibration of the high-pressure apparatus to beyond the barium transition at 80,000 atm. The resistance decrease associated with the bismuth VI-to-VIII transition at 120,000 atm was observed during experiments to 150,000 atm of pressure. At the higher pressures, tensile rupture of the central insert of the apparatus occurred.

Temperature calibration of a smaller (1/16 in. in diameter) platinum heater was undertaken. The smaller heater was employed to reduce temperature gradients existing in larger diameter heaters. Following calibration, samples of U_3O_8 were subjected to various pressures and temperatures for comparison with previously obtained results.

Part of the current investigation of the uranium-oxygen system was to determine if the cubic structure of U_4O_9 could be retained under pressure to higher oxygen content. While previous microbalance studies indicated the possibility of retaining the cubic structure to higher oxygen composition, the lattice parameter of the U_4O_9 formed under high pressure is nearly identical with that formed normally. An exception to this was observed for an early sample of U_3O_8 containing BeO. The lattice parameter of the

U_4O_9, formed by high pressure and temperature, was smaller than normal U_4O_9. As an alternative to parameter reduction by excess oxygen, it appears possible that a small amount of BeO may have entered into solid solution to produce the smaller lattice parameter. Such a reaction has not been observed to occur at normal pressure.

Work was continued on the investigation of the effect of pressure on the reaction between UO_2 and Sc_2O_3. Previous work at normal pressure had shown that Sc_2O_3 does not react with UO_2 but does with U_3O_8. Samples of UO_2 and Sc_2O_3 subjected to various pressures at temperatures above 1000 C have shown limited reaction to form a small amount of a solid solution. The parameter of the solid solution is dependent upon the temperature of the reaction. The smallest parameter observed to date, at 5.24 A, is larger than the 5.13 A resulting when the same composition is reacted in the oxidized state as U_3O_8. It cannot be concluded, however, that pressure has increased the solubility of Sc_2O_3 in UO_2 until it is established that internal oxidation did not occur during the high-pressure experimentation. Even minor oxidation of the UO_2 may markedly increase the solubility of Sc_2O_3 as it does MgO. (It has, however, been established that pressure tends to effect the reduction of the higher oxides of uranium at temperatures above 800 C).

Work will continue to complete the study of the effect of pressure on the uranium-oxygen system. Emphasis will be increased in the study of the effect of pressure on the reactions of uranium oxide with other oxides. Design improvements to achieve even higher pressures in the pressure apparatus will be incorporated, and further confirmation of the bismuth VI-to-VIII transition will follow.

Irradiation-Surveillance Program on Type 347 Stainless Steel

W. E. Murr, F. R. Shober, J. E. Howes, and J. F. Lagedrost

A surveillance program, concerned with the effects of irradiation on mechanical properties of AISI Type 347 stainless steel, is in progress. In the program, capsules containing tensile, cyclic-strain fatigue, and impact specimens are being exposed to fast-neutron irradiation (neutron energies greater than 1 Mev). One group of specimens will be irradiated at process-water temperatures (120 F) and examined at room temperature. Another group will be irradiated at 210 F, annealed at 600 F, and examined at room temperature. The third group of specimens will be irradiated near 600 F and examined at room temperature. The purpose of the program is to provide backup information on the effect of increasing neutron irradiation on the mechanical properties of Type 347 stainless steel to insure that the KAPL C-33 loop and other loops of this material are properly designed and safe for continued in-pile operation. It is estimated that the KAPL loop will operate for a period of 3 years, accumulating an integrated fast-neutron flux of between 1.4 and 1.8×10^{22} nvt. At the present time no data on the effects of irradiation on mechanical properties in Type 347 stainless steel are available for exposures greater than 3.76×10^{21} nvt; consequently, the aim of this program is to provide information with regard to the properties of stainless steel near the ultimate exposure level of the KAPL loop.

Eight capsules containing impact, fatigue, and tensile specimens have been irradiated continuously in the ETR since June, 1958. Three capsules to be irradiated at

120 F and annealed prior to testing have been operating in the ETR since August 15, 1959. The total neutron accumulation on both groups of capsules is shown on Table F-1. The last two cycles, 21 and 22, were not regular cycles and were equivalent to only 6 days at full reactor power. During Cycle 22, an additional fuel element was added to the L-10 area of the ETR core, resulting in increased instantaneous fluxes in the region of the surveillance capsules. Flux monitoring in the region of the capsules is planned to determine the new instantaneous flux values. All eleven of the surveillance capsules currently inserted in the L-10 position do not have verified reactor space after January, 1960. However it is expected that they will be allowed to remain in-pile until they reach the exposures originally scheduled, although they may be transferred to other positions within the reactor. The series of capsules designed to operate at a temperature of 600 F due to gamma heating of specimens and capsule components have been recalled from the ETR, since it does not appear that there is a chance for them to be placed in-pile in the foreseeable future. It is hoped that arrangements can be made to insert a lead capsule in the WTR at the time the reactor is being brought up to the 60-Mev operating level, to determine the suitability of the reactor space for the 600 F irradiations. In this way, the temperature and other operating characteristics of the capsule can be determined.

Development of Niobium-Base Alloys

J. A. DeMastry, F. R. Shober, and R. F. Dickerson

High strength at elevated temperatures (800 C) and comparative inertness to sodium at these temperatures make niobium alloys particularly suitable as materials for cladding applications in the EBR. At present, a vanadium-10 w/o titanium-1 w/o niobium alloy has shown acceptable properties for EBR use. The properties of the several niobium-base alloys being developed are to be compared to the vanadium-base alloy. The materials under study include unalloyed niobium and niobium-1.83 w/o chromium, niobium-3.21 w/o chromium, niobium-4.33 w/o zirconium, niobium-9.95 w/o tantalum-3.31 w/o chromium, niobium-39.8 w/o titanium-10.6 w/o aluminum, niobium-20.5 w/o-titanium-4.28 w/o chromium, and vanadium-11.7 w/o titanium-3.07 w/o niobium alloys.

All alloys being studied were forged at 2500 F in evacuated molybdenum cans. Rolling at 75 F was attempted. The niobium-1.83 w/o chromium, niobium-4.33 w/o zirconium, niobium-20.5 w/o titanium-4.28 w/o chromium, and vanadium-11.7 w/o titanium-3.07 w/o niobium alloys were reduced by cold rolling approximately 80 per cent, but showed severe edge cracking and surface defects. Tensile specimens cut from this sheet indicate that the strength of the niobium-base alloys is superior to that of the vanadium-base alloy at 1470 F.

Analysis of the unalloyed niobium showed that it had been contaminated by oxygen (increase from 200 to 820 ppm) which would account for its failure to fabricate cold in initial experiments. There was not significant increase in oxygen content of the other alloys, indicating that a higher working temperature (after initial breakdown at 2500 F) might be in order. Sections cut from the as-forged slab of each alloy were warm rolled at 800 F, and all alloys excepting the niobium-39.8 w/o titanium-10.6 w/o aluminum and niobium-9.95 w/o tantalum-3.31 w/o chromium alloys (both fractured during rolling; were

TABLE F-1. CAPSULES PREPARED FOR THE TYPE 347 STAINLESS STEEL IRRADIATION-SURVEILLANCE PROGRAM

Capsule	Type of Specimens in Capsules	Proposed Irradiation Temperature, F	Approximate Removal Date[a]	Approximate Exposure at Time of Removal[b], nvt	Total Exposure as of November 9, 1959, nvt		Location	Remarks
					Top	Bottom		
BMI-24-1	Tensile and fatigue	600	January, 1959	1.55×10^{20}	--	--	BMI	Examined at BMI Hot-Cell Facility for melting
BMI-24-2	Tensile and fatigue	120	January, 1962	1.31×10^{22}	3.041×10^{21}	3.881×10^{21}	ETR K-8-NE	Being irradiated
BMI-24-3	Tensile and fatigue	600	--	--	--	--	ETR	To be irradiated
BMI-24-4	Tensile and fatigue	120	January, 1963	1.78×10^{22}	2.123×10^{21}	3.379×10^{21}	ETR K-8-SE	Being irradiated
BMI-24-5	Tensile and fatigue	600	--	--	--	--	ETR	To be irradiated
BMI-24-6	Tensile and fatigue	120	June, 1961	1.08×10^{22}	4.004×10^{21}	3.116×10^{21}	ETR K-8-NE	Being irradiated
BMI-24-7	Tensile and fatigue	600	--	--	--	--	ETR	To be irradiated
BMI-24-8	Tensile and fatigue	120	June, 1962	1.54×10^{22}	2.380×10^{21}	3.447×10^{21}	ETR K-8-SE	Being irradiated
BMI-24-9	Tensile and fatigue	600	--	--	--	--	ETR	To be irradiated
BMI-24-10	Tensile and fatigue	120	January, 1961	0.84×10^{22}	3.325×10^{21}	3.400×10^{21}	ETR K-8-SE	Being irradiated
BMI-24-11[c]	Tensile and fatigue	600	--	--	--	--	ETR	Damaged at ETR
BMI-24-12	Tensile and fatigue	120	June, 1960	0.61×10^{22}	4.330×10^{21}	3.724×10^{21}	ETR L-8-SE	Being irradiated
BMI-24-13	Impact	600	--	--	--	--	ETR	To be irradiated
BMI-24-14	Impact	120	June, 1962	1.54×10^{22}	3.759×10^{21}	3.834×10^{21}	ETR K-8-NW	Being irradiated

TABLE F-1. (Continued)

Capsule	Type of Specimens in Capsules	Proposed Irradiation Temperature, F	Approximate Removal Date[a]	Approximate Exposure at Time of Removal[b], nvt	Total Exposure as of November 9, 1959, nvt		Location	Remarks
					Top	Bottom		
BMI-24-15	Impact	600	--	--	--	--	ETR	To be irradiated
BMI-24-16	Impact	120	June, 1960	0.61×10^{22}	3.807×10^{21}	3.460×10^{21}	ETR K-8-NW	Being irradiated
BMI-24-17[c]	Tensile and fatigue	600	October, 1958	3.25×10^{20}	--	--	BMI	Examined at BMI Hot-Cell Facility after high temperature observed
BMI-24-18	Tensile and fatigue	120	--	--	3.81×10^{20}	6.06×10^{20}	ETR	Being irradiated for postirradiation annealing studies
BMI-24-19[c]	Tensile and fatigue	600	--	--	--	--	ETR	Fabricated to replace BMI-24-17
BMI-24-20	Tensile and fatigue	120	--	--	3.76×10^{20}	6.92×10^{20}	ETR	Being irradiated for postirradiation annealing studies
BMI-24-21	Tensile and fatigue	600	--	--	--	--	ETR	Fabricated to replace BMI-24-1
BMI-24-22	Tensile and fatigue	120	--	--	4.92×10^{20}	8.21×10^{20}	ETR	Being irradiated for postirradiation annealing studies

(a) Based on 6-month lead on loop, plus 2 months for examination.
(b) Based on maximum fast flux at tube of 1.7×10^{14} nv for 6-month periods.
(c) Thermocouple lead capsule.

successfully reduced about 70 per cent. After this second breakdown of structure, the rolled sheet was cut into three pieces and cold-rolling studies were conducted. One piece of each alloy was cold rolled with no further treatment. This rolling was successful, but the sheet exhibited edge cracking, and the surfaces were poor. A second piece was belt sanded to remove surface defects and edge cracks. This piece was then cold rolled and yielded much better appearing sheet than that which had no prior surface conditioning. Results of rolling are shown in Table F-2. The third piece of sheet was belt sanded and annealed for 1 hr at 2550 F and furnace cooled. The results shown in Table F-3 indicate that this treatment produced the best sheet. Fabrication of the contaminated unalloyed niobium which had been surface conditioned and annealed in this manner resulted in sheet which had no edge cracks or surface defects. The effect of annealing (2550 F for 1 hr) on the hardness of sheet rolled at 800 F is shown in Table F-4.

Additional ingots of alloys which were successfully fabricated by warm rolling at 800 F are being prepared. These ingots will be fabricated, tensile properties will be determined, and sheet-to-sheet weldability studies will be made.

Development of Corrosion-Resistant Niobium Alloys

D. J. Maykuth, W. D. Klopp, E. F. Adkins,
R. I. Jaffee, W. E. Berry, and F. W. Fink

The evaluation of selected niobium-base alloys for service in pressurized-water reactors was continued. Earlier work has shown that binary niobium-vanadium alloys offer the greatest advantage as a base material over the other binary-alloy systems investigated. The current studies are concerned with optimizing alloy compositions to improve fabricability while maintaining adequate hot strength and corrosion resistance.

Corrosion results obtained to date for all alloys tested are summarized in Table F-5. The results continue to indicate that:

(1) Unalloyed niobium is not sufficiently resistant in high-temperature water to warrant its use as a cladding material.

(2) Additions of titanium, vanadium, or zirconium markedly improve the corrosion resistance of niobium.

(3) The most corrosion-resistant alloys are those containing more than 45 a/o zirconium or a ternary containing 28 a/o titanium-6 a/o chromium.

(4) A 12 a/o vanadium alloy possesses the optimum combination of high-temperature strength, low cross section, and adequate corrosion resistance.

(5) Ternary additions on the order of 5 a/o to niobium-vanadium alloys do not result in increased corrosion resistance.

TABLE F-2. FABRICATION OF SURFACE PREPARED NIOBIUM-BASE ALLOYS

Material cut from slabs forged at 2500 F.

	Results of Fabrication Experiments			
	Rolled at 800 F Without Surface Preparation		Rolled at 75 F With Surface Belt Sanded to Remove Cracks and Warm-Rolling Overlaps	
Alloy Composition, w/o	Reduction, per cent	Remarks	Reduction[a], per cent	Remarks
Niobium	67	Surface cracks, edge cracks	62	Rough edge, occasional surface cracks
Nb-1.83 Cr	70	Slight edge cracks	80	Slightly rough edge, bright, clear surface
Nb-3.21 Cr	77	Slight edge cracks, surface cracks	70	Occasional edge cracks, no surface cracks
Nb-4.33 Zr	74	Rough edges, no surface cracks	75	No edge cracking, no surface cracks
Nb-20.5 Ti-4.28 Cr	80	Rough edges, no surface cracks	72	No edge cracking, no surface cracks
V-11.7 Ti-3.07 Nb	73	Edge cracks, slight surface cracks	75	Edge cracks no surface cracks

(a) Reduction is calculated from thickness of sheet rolled at 800 F and is not total reduction from ingot. Total reduction is above 95 per cent for all alloys.

F-9

TABLE F-3. FABRICATION OF SURFACE-PREPARED ANNEALED NIOBIUM-BASE ALLOYS

Material cut from slabs forged at 2500 F.

	Results of Fabrication Experiments			
	Rolled at 800 F Without Surface Preparation		Rolled at 75 F With Surface Belt Sanded After Annealing 1 Hr at 2550 F and Furnace Cooling	
Alloy Composition, w/o	Reduction, per cent	Remarks	Reduction[a], per cent	Remarks
Niobium	67	Surface cracks edge cracks	80	No edge cracks no surface cracks
Nb-1.84 Cr	70	Slight edge cracks	80	Smooth edges
Nb-3.21 Cr	77	Slight edge cracks, surface cracks	80	Rare edge cracks, no surface cracks
Nb-4.33 Zr	74	Rough edges, no surface cracks	80	Smooth edges
Nb-20.5 Ti-4.28 Cr	80	Rough edges, no surface cracks	81	Smooth edges
V-11.7 Ti-3.07 Nb	73	Edge cracks, slight surface cracks	80	Rough edges, no surface cracks

(a) Reduction is calculated from thickness of sheet rolled at 800 F and is not total reduction from ingot. Total reduction is above 95 per cent for all alloys.

TABLE F-4. EFFECT OF ANNEALING FOR 1 HR AT 2550 F ON HARDNESS OF NIOBIUM-BASE ALLOYS

	Rockwell A Hardness (50-Kg Load)	
Alloy Composition, w/o	After Rolling at 800 F	Annealing 1 Hr at 2550 F and Furnace Cooling
Niobium	55	39
Nb-1.83 Cr	62	53
Nb-3.21 Cr	68	60
Nb-4.33 Zr	58	46
Nb-20.5 Ti-4.28 Cr	65.5	64
V-11.7 Ti-3.07 Nb	64	56

F-10

TABLE F-5. SUMMARY OF CORROSION RESULTS OBTAINED ON NIOBIUM ALLOYS EXPOSED TO HIGH-TEMPERATURE WATER AND STEAM

Alloy Addition (Balance Niobium), a/o	600 F Water		680 F Water		750 F Steam	
	Exposure Time, days	Total Weight Change, mg per cm^2	Exposure Time, days	Total Weight Change, mg per cm^2	Exposure Time, days	Total Weight Change, mg per cm^2
			Commercial Niobium, Rocking-Hearth Melts			
Unalloyed Nb	252	-35.0[b]	42[a]	Disintegrated	28[a]	Disintegrated
10.5 Zr	--	--	196[a]	0.67	140	-21.8
26.1 Zr	--	--	196[a]	0.07	--	--
35.7 Zr	--	--	196[a]	0.66	--	--
45.7 Zr	--	--	196[a]	0.55	--	--
1.08 W	--	--	196[a]	-2.60	140	-28.7
4.67 W	--	--	196[a]	-29.3	--	--
9.56 W	--	--	7[a]	Cracked	--	--
2.45 Mo	--	--	196[a]	-7.10	98	Disintegrated in 98 days
5.20 Mo	--	--	196[a]	-1.30	140	-81.5
7.40 Mo	--	--	196[a]	0.62	--	--
4.42 V	--	--	196[a]	0.42	140	-4.03
6.59 V	--	--	196[a]	0.73	140	1.23
8.93 V	--	--	196[a]	0.59	140	1.04
10.7 V	--	--	196[a]	0.78	--	--
13.7 V	--	--	196[a]	0.50	--	--
24.2 V	--	--	196[a]	0	--	--
4.90 Fe	--	--	196[a]	0.10	98	Disintegrated in 98 days
9.41 Ti	--	--	196[a]	0.65	140	1.27
18.8 Ti	--	--	196[a]	0.48	--	--
24.3 Ti	--	--	196[a]	0.52	--	--
30.5 Ti	--	--	196[a]	0.40	--	--
33.8 Ti	--	--	196[a]	0.33	--	--
12.0 Ti-0.5 Cr	--	--	196[a]	0.66	--	--
20.2 Ti-2.1 Cr	--	--	196[a]	0.39	--	--
28.2 Ti-6.1 Cr	--	--	196[a]	0.20	--	--
12.0 Ti-4.2 Mo	--	--	196[a]	0.64	--	--
17.4 Ti-6.2 Mo	--	--	196[a]	0.54	--	--
23.1 Ti-7.8 Mo	--	--	196[a]	0.45	--	--
10.4 Ti-5.0 V	--	--	196[a]	0.56	--	--
16.1 Ti-8.4 V	--	--	196[a]	0.40	--	--
22.6 Ti-11.0 V	--	--	196[a]	0.48	--	--

F-11

TABLE F-5. (Continued)

Alloy Addition (Balance Niobium), a/o	600 F Water Exposure Time, days	600 F Water Total Weight Change, mg per cm^2	680 F Water Exposure Time, days	680 F Water Total Weight Change, mg per cm^2	750 F Steam Exposure Time, days	750 F Steam Total Weight Change, mg per cm^2
High-Purity Niobium, Consumable-Electrode Melts						
Unalloyed Nb	252	0.89	224	-5.47	224	-54.0
7.18 Mo	252	0.80	224	-0.96	70[a]	Cracked
12.5 V	252	0.45	224	0.58	224	0.80
46.8 Zr-5.06 Ti	224	0.30	196	0.92	196	2.60
11.2 Ti-3.2 Mo	224	0.46	196	0.54	196	0.62
18.8 Ti-8.7 Mo	224	0.26	196	0.53	196	0.60
9.9 Zr-9.4 V	112	0.12	112	0.35	112	-2.47
5.7 Zr-11.4 V	112	0.13	112	0.30	112	-0.74
9.1 Ti-6.3 Cr	112	0.09	112	0.36	112	-2.64
High-Purity Niobium, Rocking-Hearth Melts						
Unalloyed Nb	--	--	140	0.92[b]	--	--
Unalloyed Nb	--	--	84[a]	Disintigrated in 84 days	--	--
Unalloyed Nb	--	--	112	0.58[b]	--	--
1.1 Zr	--	--	140	-204.0	--	--
2.2 Zr	--	--	56	-12.6	--	--
5 Zr	--	--	112	-6.56	--	--
10.2 Zr	--	--	112	-0.18	--	--
40 Zr	--	--	112	0.54	--	--
65 Zr	--	--	112	0.62	--	--
75 Zr	--	--	112	0.78	--	--
90 Zr	--	--	112	0.93	--	--
3.2 Ti	--	--	140	-2.86	--	--
10.5 Ti	--	--	140	0.59	--	--
25.0 Ti	--	--	140	0.39	--	--
<0.02 Cr	--	--	140	0.74[b]	--	--
0.5 Cr	--	--	140	0.37[b]	--	--
0.5 Cr	--	--	112	-1.71	--	--
<0.08 Fe	--	--	112	-0.83	--	--
0.3 Fe	--	--	56	-7.40	--	--
10 Fe	--	--	28[a]	-20.0	--	--

F-12

TABLE F-5. (Continued)

Alloy Addition (Balance Niobium), a/o	600 F Water		680 F Water		750 F Steam	
	Exposure Time, days	Total Weight Change, mg per cm^2	Exposure Time, days	Total Weight Change, mg per cm^2	Exposure Time, days	Total Weight Change, mg per cm^2
10.9 Zr-5.1 Ti	--	--	112	0.50	--	--
25 Zr-5 Ti	--	--	112	0.10[b]	--	--
25 Zr-15 Ti	--	--	112	0.48	--	--
25 Zr-25 Ti	--	--	112	0.34	--	--
35 Zr-5 Ti	--	--	112	0.48	--	--
35 Zr-15 Ti	--	--	112	0.43	--	--
45 Zr-5 Ti	--	--	112	0.52	--	--
10 Zr-5 Mo	--	--	112	0.16	--	--
35 Zr-5 Mo	--	--	112	0.44	--	--
45 Zr-5 Mo	--	--	112	0.47	--	--
35 Zr-5 Al	--	--	112	0.35	--	--
45 Zr-5 Al	--	--	112	0.51	--	--
10 Zr-5 Cr	--	--	112	0.46	--	--
45 Zr-5 Cr	--	--	112	0.39	--	--
10 Zr-5 Fe	--	--	112	0.24	--	--
2.5 V	--	--	140	0.63	--	--
2.0 V-2.5 Ti	--	--	112	0.64	--	--
2.0 V-2.3 Mo	--	--	112	0.79	--	--
2.2 V-0.54 Fe	--	--	112	0.67	--	--
1.8 V-<0.02 Cr	--	--	112	0.52	--	--
1.8 V-0.14 Al	--	--	112	0.79	--	--
2.5 V-2.5 Zr	--	--	56	-1.21	--	--
2.2 V-0.87 Ni	--	--	28[a]	-1.00	--	--
4.0 V-2.3 Zr	--	--	112	0.46	--	--
5 V-25 Zr	--	--	112	-0.35	--	--
2.5 V-35 Zr	--	--	112	0.24[b]	--	--
5 V-45 Zr	--	--	112	0.42	--	--
10 Zr	--	--	--	--	14	0.36
10 Ti	--	--	--	--	14	0.33

(a) Off test.
(b) Losing weight.

F-13

The cooperative corrosion testing program with the Knolls and Bettis Laboratories is continuing. Results after 98 days of exposure reveal average weight changes of +84.4 mg per cm^2 in 680 F water and -844 mg per cm^2 in 750 F 1550-psi steam. Specimens in 680 F water are slowly losing weight after a peak weight gain of 121 mg per cm^2 at 42 days of exposure. Specimens exposed to 750 F steam began to lose weight after 28 days of exposure and have continued to lose weight at an erratic rate.

Corrosion tests are continuing on all of the alloy specimens except those noted in Table F-5. Corrosion tests have been started in 680 F water on specimens from the 50-g alloy ingots described below. No results are available to date.

Niobium-1 a/o cerium
Niobium-1 and -5 a/o yttrium
Niobium-1 a/o palladium
Niobium-5 a/o vanadium-2.5 a/o titanium
Niobium-5 a/o vanadium-2.5 a/o chromium
Niobium-5 a/o vanadium-2.5 a/o aluminum

Fabrication was completed on the 25 screening alloy ingots. The compositions are listed in Table F-6 along with cast hardness and fabrication conditions. Cerium and yttrium additions up to 5 a/o act as very strong deoxidizers during melting with the result that arc-melted alloys containing these additions are as soft as or softer than the niobium base (as-received hardness of 81 VHN) used in their preparation. Cerium and yttrium also markedly lower the surface tension of molten niobium, making it difficult to obtain button-shaped ingots in arc melting, and an alloy charge containing 5 a/o cerium could not be coalesced into a useful ingot shape.

Generally, fabrication by cold rolling was attempted for all ingots with a hardness of 150 VHN or less, while the harder ingots were pack rolled in evacuated stainless steel cans at 1800 F. As indicated in Table F-6, each of the ingots, except those containing 2.5 a/o and 5 a/o nickel, were successfully rolled to sound 60-mil-thick strip by either of these procedures. Even from these two alloys, however, sufficient sound strip was salvaged to prepare duplicate corrosion-test samples for exposure to 680 F water. Corrosion-test samples of each of these alloys will be prepared after the hot-rolled strips have been cleaned up by surface grinding, and all of the strips have been vacuum annealed for 1 hr at 1200 C (2190 F).

Double, consumable-electrode arc melting was completed on the four 2-1/2-lb ingots for which compositions and hardnesses are indicated below:

Alloy	Nominal Alloy Composition, a/o	Bhn (1500-Kg Load)
NL-11	Nb-7.5 V	168
NL-12	Nb-7.5 V-0.19 N[(a)]	182
NL-13	Nb-7.5 V-2.5 Ti	172
NL-14	Nb-7.5 V-2.5 Mo	185

(a) Equivalent to 0.03 w/o nitrogen.

TABLE F-6. COMPOSITIONS, HARDNESSES, AND FABRICATION DATA FOR 50-G INGOTS OF NIOBIUM-BASE SCREENING ALLOYS

Alloy	Nominal Alloy Content (Balance Niobium), a/o	As-Cast Hardness, VHN	Rolling Temperature, F[a]	Remarks
N56	100 Nb	93	75	--
N57	1 Ce	73	75	--
N58	5 Ce	--	--	Could not be melted to useful-shaped ingot
N59	1 Y	86	75	--
N60	5 Y	67	75	--
N61	1 Ni	140	1800	Cracked during attempted cold rolling
N62	2.5 Ni	192	1800	One end cracked during hot rolling
N63	5 Ni	223	1800	Strip broke into three pieces during hot rolling
N64	1 Pd	107	75	--
N81	5 V	159	75	--
N65	5 V-2.5 Ti	150	75	--
N66	5 V-2.5 Mo	164	1800	--
N67	5 V-2.5 Fe	177	1800	--
N68	5 V-2.5 Cr	149	75	--
N69	5 V-2.5 Ni	232	1800	--
N70	5 V-2.5 Al	150	75	--
N71	2.5 V-0.5 C	153	1800	--
N72	5 V-0.5 C	198	1800	--
N73	2.5 V-0.25 Ti-0.50	162	1800	--
N74	5 V-0.25 Ti-0.5 O	179	1800	--
N75	2.5 V-0.25 Zr-0.5 O	165	1800	--
N76	5 V-0.25 Zr-0.5 O	188	1800	--
N77	2.5 V-0.5 Ti-0.5 C	150	1800	--
N78	5 V-0.5 Ti-0.5 C	199	1800	--
N79	2.5 V-0.5 Zr-0.5 C	160	1800	--
N80	5 V-0.5 Zr-0.5 C	203	1800	--

(a) Alloys rolled at 75 F were rolled bare. Alloys rolled at 1800 F were canned in evacuated stainless steel packs.

These ingots have been cut into slabs which are being sealed in evacuated stainless steel cans for pack rolling at 1800 F. After fabrication and annealing, samples of each alloy will be corrosion tested in 600 F and 680 F water and 750 F steam, and will be evaluated in room- and elevated-temperature tensile and creep tests as well.

Investigation of the Creep Properties of Zircaloy-2 During Irradiation at Elevated Temperatures

F. R. Shober, P. B. Shumaker, A. P. Young, M. F. Amateau, and R. F. Dickerson

An investigation of the creep properties of Zircaloy-2 during irradiation at elevated temperatures has been undertaken. The purpose of this investigation is to compare the deformation obtained in Zircaloy-2 under stress during irradiation with the deformation obtained in Zircaloy-2 under conventional testing at the same stresses. A part of the program includes studies to detect and describe the strain-aging phenomenon which has been detected in nonirradiated Zircaloy-2. If strain-aging is detected, then a study of its mechanism and its influence on creep properties at elevated temperature during irradiation will be made.

The design of capsules for the irradiation of Zircaloy-2 specimens subjected to tensile load during in-pile exposure is partially completed. The capsule design is based on a 30-mil-thick flat-strip specimen attached to a bellows which is to be loaded by a helium pressure within the capsule. Each specimen will have the three gage sections of different widths, the smallest being about 5/16-in. wide. A stress of approximately 25,000 psi will be achieved at this section by a gas pressure on the bellows of 500 psi.

The specimen temperature during irradiation will be 650 F and will be maintained by a combination of gamma heat and heat supplied by sheathed resistance heaters incorporated into the capsule system. The output of these heaters will be controlled by thermocouples located in a narrow gap between a stressed specimen and an unstressed specimen parallel with it. The latter specimen will be present to provide thermal symmetry about the capsule axis (both the stressed and unstressed specimens will be offset from the capsule axis about 35 mils). Since there should be virtually no temperature gradient across the gap, the thermocouple temperatures should be quite close to the specimen temperatures.

At present, effort is concentrated on designing the bellows and specimen attachments. The basic unit will be a welded-metal bellows since it has a relatively low spring-rate characteristic and, consequently, can undergo fairly large deformations without producing large spring forces.

During the next few weeks, the irradiation-capsule design will be completed, and the fabrication of out-of-pile systems similar to the in-pile systems will be inaugurated. Initially, out-of-pile experiments will be conducted to check out the various components of the in-pile systems; at a later date, out-of-pile experiments will furnish creep data for comparison with those obtained from hot-cell examinations of the irradiated specimens.

F-16

A portion of the strain-aging studies has been started. Sheet-type tensile specimens have been prepared. Room- and elevated-temperature tensile tests to detect strain aging will be made with these specimens. These preliminary studies will be repeated when a second lot of Zircaloy-2 is available. Internal-friction studies of unaged Zircaloy-2 have been made to establish data for comparison with strain-aged material. A peak detected in the internal-friction curve at 280 C on material annealed at 750 C and furnace cooled was increased slightly by straining the Zircaloy-2 approximately 2 per cent. It was thought that the peak at 280 C was associated with the mobility of solute atoms. In order to amplify this effect, internal-friction tests were made over the temperature range 25 to 500 C on material annealed at 750 C for 1 hr and water quenched. The peak was magnified and the internal friction for two consecutive runs was higher by a factor of 10 than that obtained on the annealed or the cold-worked material. The 280 C peak presumably represents a relaxation process which involves atomic diffusion. A relaxation process which produces an internal-friction peak at 280 C should be rapid enough to account for strain aging at 350 C.

The study of thin films of zirconium and Zircaloy-2 by electron transmission has continued. Thin sections are being prepared from bulk materials instead of rolled sheet. The high degree of preferred orientation of the rolled sheet has prevented study of slip on the prismatic planes of zirconium. Slip occurs in zirconium predominantly on these prismatic planes. Dislocation networks associated with slip can be more easily detected in the bulk material. Techniques to reduce the bulk material to thin sheet for electron microscopy are being studied. The detection of the dislocations and their interactions is expected to aid in the strain-aging studies.

Determination of Oxygen in Sodium at Concentrations Below 10 PPM

D. Ensminger, D. R. Grieser, E. H. Hall,
J. W. Kissel, J. McCallum, and W. H. Goldthwaite

Investigations are being made to establish the feasibility of continuously monitoring the oxygen content of large sodium systems at concentrations below 10 ppm. Although plugging indicators have been successfully applied at higher concentration levels, predicted sensitivity at 10 ppm and below appears low. Accordingly, additional techniques are being studied in order to establish their feasible application to the rapid analysis of sodium for oxygen in low concentrations with the desired sensitivity of ±1 ppm.

Initial evaluations are to be made at oxygen levels in the 20 to 100-ppm range. This will permit the establishment of general applicability and provide results which can be extrapolated to the desired working range, but will avoid the difficult handling and sampling problems during the early stages of the program. The more promising of these techniques will then receive additional study using sodium containing low levels of oxygen.

Ellipsometry

The technique of ellipsometry utilizes a polarizing spectrometer to measure certain optical properties of reflecting surfaces. Although the optical properties of sodium have been previously studied by this technique, no attempt was made to determine the effect of oxygen content on the measurements.

In the present investigation sodium samples containing differing oxygen contents will be examined to determine the degree of correlation between concentration and the measured ellipticity and rotation of the plane of the reflected light. The temperature of the sodium is to be maintained above a level sufficient to keep all of the contained oxygen in solution. Several Pyrex cells for holding the sodium samples have been fabricated, and the investigation will begin when sodium samples become available.

Electrical Resistivity

A device has been designed which will be used to measure the effect of oxygen content upon the apparent electrical resistivity of sodium. This consists of a small, thin-walled, hypodermic tube through which the sodium can be flowed. Electrodes on the tube will permit the measurement of the resistance. Electric heaters surrounding the resistance tube will be used to maintain the apparatus above the oxygen-saturation temperature. The device is at present in the fabrication stage and when completed will be incorporated into the sodium-purification loop for the evaluations.

Polarographic Studies

As one possible means for measuring oxygen content in sodium, the physics and electrochemistry of sodium drops are being studied. The work has been started with a Pyrex system, which will be used to measure sodium-drop rates as a function of temperature and oxygen content. The first setup was made during November, and was checked out with water. During December, the following work is planned:

(1) Perform final calibration of the capillary system.

(2) Measure drop rates of two sodium samples having different oxygen contents.

(3) Construct an inverted setup for rising drops into a fused salt.

(4) Check feasibility for electrochemically titrating oxygen in sodium.

Mass Spectrographic Study

The feasibility of a mass spectrometric method of analysis for oxygen in sodium is to be studied by the total vaporization of a small known quantity of sodium within the ion source of a mass spectrometer. The ion current produced by the most abundant

species of sodium oxide ion is to be integrated over the total time of vaporization. The integrated ion current may then be compared with that obtained for a standard sodium sampling having a known oxygen content.

The first phase of this work will be the design and construction of equipment to (1) meter the sodium into the mass-spectrometer vaporizer, and (2) integrate the ion currents obtained.

Concurrently, an electron multiplier is to be incorporated in the detection system of the mass spectrometer in order to obtain the high sensitivity necessary for this study.

Plugging-Indicator Studies and Purification Loop

A sodium loop is being constructed for the production of sodium with controlled oxygen levels. Samples for the various evaluation programs will be furnished from this purification train. A vacuum-distillation apparatus will be used as the standard calibration technique for oxygen determination.

A plugging indicator with an improved type temperature control will be incorporated into the purification train so that its performance may be evaluated. The fabrication of the train has been virtually completed so that samples can be prepared and furnished to the other evaluation studies in this program. Evaluation runs of the plugging indicator will also be made.

STUDIES OF ALLOY FUELS

R. F. Dickerson

Niobium-base binary alloys containing uranium in amounts between 10 and 60 w/o have been removed from corrosion test after 140 days in 680 F water and analyzed for hydrogen contamination. The results of these analyses show that the hydrogen pickup varies inversely with the uranium content. A 1000-hr corrosion test in NaK at 1600 F has been completed, and all alloys appear to be comparatively inert to attack. Alloys to be used in the study of the effect of oxygen on the gamma loop have been cast and are being homogenized.

Thorium-base ternary alloys containing 15 w/o uranium-25 w/o zirconium and 10 w/o uranium-25 w/o zirconium exhibit corrosion rates of less than 0.75 mg/(cm^2)(hr) after a 168-hr exposure in 200 C water. These alloys were designed to have a continuous network of delta phase around the thorium and thus provide additional corrosion resistance. The desired structure was not obtained, and, consequently, very little improvement in corrosion resistance was noted. Carbon and yttrium additions have been made to thorium and binary alloys in an attempt to improve high-temperature strength. Attempts to prepare $ThN_{1.0}$ by arc melting are being continued.

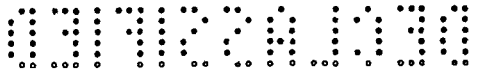

F-19

A program concerned with a study of plutonium alloys has been planned, and active research will be initiated upon completion of the Battelle Plutonium Facility. This program was discussed briefly in BMI-1391 and will not be reported again until the experimental studies have begun.

Development of Niobium-Uranium Alloys

J. A. DeMastry, S. G. Epstein, A. A. Bauer, and R. F. Dickerson

As a means of developing and evaluating niobium-uranium alloys as reactor fuels the fabrication characteristics, mechanical and physical properties, and corrosion behavior in various environments of these alloys are being investigated.

Alloys containing from 10 to 60 w/o uranium have been prepared using niobium containing from 0.03 to 0.07 w/o oxygen and from 0.02 to 0.74 w/o zirconium. The fabrication characteristics, tensile properties, and corrosion behavior in NaK, water, steam, air, and CO_2 were determined using the above materials. No effects were found on the above-mentioned properties as a result of variations in the oxygen and zirconium contents of the alloys examined in the study.

Alloys containing 30 w/o or more uranium have not been successfully fabricated to date. Ingots of niobium-30, -40, and -50 w/o uranium have been prepared for fabrication attempts at 3000 F.

Corrosion tests of niobium-uranium alloy specimens in water at 680 F have been discontinued after 140 days, and the specimens have been analyzed for hydrogen content. The analyses were performed on corrosion specimens with unabraded surfaces by vacuum-fusion techniques. The amount of hydrogen picked up during testing was high for the alloys containing 10 w/o uranium and decreased as the uranium content increased. Table F-7 shows the results of these analyses.

Corrosion tests of niobium-uranium alloys in 600 F water have continued through 168 days with no apparent changes in corrosion behavior. All specimens still have a black oxide and most show a net positive weight change even though almost all are now losing weight. The results after 154 and 168 days of testing are shown in Table F-8.

A 1000-hr corrosion test of niobium-uranium alloys in NaK at 1600 F has been completed. All alloys appear to be comparatively inert to attack by NaK. The weight changes observed are probably due to pickup of oxygen present as a contaminant in the NaK. Additional oxygen is introduced each time the capsules are opened and the NaK is changed. The results of testing are shown in Table F-9.

Specimens which were recovered after testing in NaK have been machined to remove surface oxide. The specimens are being re-encapsuled in stainless steel tubes containing sodium for testing at 1500 F.

One-hundred-hour stress-rupture tests of niobium-10 and -20 w/o uranium alloys are in progress.

TABLE F-7. RESULTS OF ANALYSIS[a] FOR HYDROGEN CONTENT OF NIOBIUM-URANIUM ALLOYS AFTER 140 DAYS IN 680 F WATER

Nominal Composition (Balance Niobium), w/o	Analyzed Oxygen Content Before Exposure, ppm	Analyzed Hydrogen Content, ppm	
		Before Exposure	After Exposure[b]
10 U	680	9	155
	1190	3	870
	3170	7	1510
20 U	458	7	89
	523	10	790
	198	19	47
30 U	586	62	127
	669	12	66
	165	39	21
40 U	661	7	52
	579	2	46
	261	7	10
50 U	375	7	28
	334	4	16
	271	2	23
60 U	471	9	66
	273	3	35
	192	3	(c)

(a) Vacuum-fusion method.
(b) Performed on unabraded surfaces.
(c) Lost in test after 70 days.

TABLE F-8. CORROSION DATA FOR NIOBIUM-URANIUM ALLOYS[a] EXPOSED IN 600 F WATER

Nominal Alloy Content (Balance Niobium), w/o	Impurity Content		Specimen Condition	Total Weight Change in 600 F Water, mg per cm^2	
	Oxygen[b], ppm	Zirconium[c], w/o		After 154 Days	After 168 Days
10 U	680	0.74	Fabricated	0.51	0.60
	1190	0.17	Fabricated	-0.15	0.59
	3170	0.02	Fabricated	-0.94	-1.52
20 U	458	0.74	Fabricated	0.94	0.98
	523	0.17	Fabricated	1.50	1.64
	198	0.02	Fabricated	0.63	0.69
30 U	586	0.74	As cast	0.62	0.53
	669	0.17	Fabricated	-0.61	-1.28
	165	0.02	As cast	0.71	0.40
40 U	661	0.74	As cast	0.43	0.49
	579	0.17	As cast	0.33	0.28
	261	0.02	As cast	0.66	0.57
50 U	375	0.74	As cast	0.63	0.61
	334	0.17	As cast	0.63	0.53
	271	0.02	As cast	0.23	0.04
60 U	471	0.74	As cast	-2.50	-3.28
	273	0.17	As cast	-2.01	-2.80
	192	0.02	As cast	-0.42	-0.76

(a) Average of duplicate specimens.
(b) Analyzed value.
(c) Nominal composition.

TABLE F-9. CORROSION DATA FOR NIOBIUM-URANIUM ALLOYS[a] EXPOSED IN NaK AT 1600 F

Nominal Alloy Content (Balance Niobium), w/o	Impurity Content		Specimen Condition	Total Weight Change in 1600 F NaK, mg per cm^2		
	Oxygen[b], ppm	Zirconium[c], w/o		After 156 Hr	After 656 Hr	After 1000 Hr
10 U	680	0.74	Fabricated	0	0.17	0.14
	1190	0.17	Fabricated	-0.66	0.05	-1.01
	3170	0.02	Fabricated	-0.33	-0.03	-0.31
20 U	458	0.74	Fabricated	0.92	0.37	1.25
	523	0.17	Fabricated	0.67	0.14	0.93
	198	0.02	Fabricated	0.31	0.25	0.69
30 U	165	0.02	As cast	0.93	0.52	2.09
40 U	261	0.02	As cast	1.48	0.38	2.51
50 U	271	0.02	As cast	0.96	0.55	2.50
60 U	192	0.02	As cast	1.36	1.15	3.24

(a) Average of duplicate specimens.
(b) Analyzed oxygen content.
(c) Nominal composition.

F-23

Alloys in wire-bar form are being homogenized prior to a study of the effects of oxygen on the composition limits of the gamma loop in the niobium-uranium system. Ternary alloys rich in uranium also have been arc melted and are ready for homogenization. These ternaries consist of niobium-60 w/o uranium-5, -10, and -20 w/o zirconium and niobium-50 w/o uranium-5, -10, and -20 w/o zirconium alloys. These compositions are being investigated in an effort to develop single-phase ternary alloys containing more uranium than is possible with binary alloys.

Development of Thorium-Uranium Alloys

M. S. Farkas, A. A. Bauer, and R. F. Dickerson

Development of thorium-uranium-base alloys with improved radiation stability and corrosion resistance is the objective of a program currently in progress. The effect of thorium purity, casting methods, and fabrication on the size and distribution of uranium-rich particles is being investigated. Alloy compositions being studied are thorium-5 to 20 w/o uranium-10 to 25 w/o zirconium in which the zirconium-to-uranium ratio is greater than one. Other compositions are thorium-uranium-base alloys with additions of niobium, molybdenum, and zirconium and niobium. The preparation and properties of thorium and thorium-uranium carbides and nitrides are also being investigated.

Metallographic examination of thorium-uranium-zirconium alloys heat treated for 24 hr at 1000 C and furnace cooled shows that particles of zirconium-uranium exist in a thorium-rich matrix. This matrix material is pearlitic in nature, a structure which is probably produced by the monotectoid reaction of the thorium-zirconium system. Also, in several alloys the particles which were zirconium-uranium solution at 1000 C exhibited small platelets of alpha zirconium which precipitated on cooling as a result of decomposition of the zirconium-uranium solid solution. Particle size after heat treatment is large compared with particle size in the as-cast state.

Corrosion tests in 200 C water are now being performed. Thorium alloys heat treated at 1000 C and either furnace cooled or water quenched have been on test for 168 hr. Of the group that was furnace cooled, the thorium-15 w/o uranium-25 w/o zirconium and thorium-20 w/o uranium-20 w/o zirconium alloys performed well with corrosion rates of less than 0.9 mg/(cm^2)(hr). Of the alloys water quenched from 1000 C, the thorium-15 w/o uranium-25 w/o zirconium and thorium-10 w/o uranium-25 w/o zirconium alloys out performed the others with average corrosion rates of less than 0.75 mg/(cm^2)(hr). The corrosion resistance of these alloys is not significantly greater than that of thorium, which is reported to be 1.5 mg/(cm^2)(hr) in 200 C water. It was hoped that the high zirconium contents in these alloys would aid in providing a continuous network of delta phase and thus improve the corrosion resistance. However, the desired structure has not been obtained; and the corrosion resistance is virtually the same as obtained on previously tested ternary and quaternary alloys containing less zirconium.

Carbon and yttrium additions have been made to thorium binary and ternary alloys in an attempt to improve their high-temperature strength. Compositions prepared are of the thorium-10 w/o uranium base with additions of 0.2 w/o carbon, 1.5 w/o molybdenum-0.2 w/o carbon, 2 w/o niobium-0.2 w/o carbon, and 10 w/o yttrium.

Hot-hardness measurements will be performed to obtain an estimate of the strengthening obtained.

Further investigations to be conducted on thorium-uranium-base alloys will include studies of the effect of heat treatment on microstructure, determination of tensile and creep properties, and studies of recrystallization behavior.

Thorium has been arc melted under a dynamic atmosphere of nitrogen maintained at about 2-1/2 atm. Analysis of the button prepared shows that 4.9 w/o nitrogen was absorbed. This is equivalent to $ThN_{0.86}$. Previous attempts to obtain stoichiometric ThN, using a 1/3-atm pressure, yielded $ThN_{0.71}$. The microstructure of the $ThN_{0.86}$ sample shows only a small amount of free thorium. Further melting studies will be conducted on the preparation of thorium-uranium nitrides.

FISSION-GAS RELEASE FROM REFRACTORY FUELS

J. B. Melehan, D. A. Vaughan, R. H. Barnes, H. Sheets,
S. D. Beck, and F. A. Rough

Various studies are being directed toward understanding the causes of gas release in uranium dioxide. In this program characterization of sintered UO_2 and out-of-pile diffusion of fission gases and in-pile fission-gas release from UO_2 are under investigation.

Characterization of Sintered UO_2 and Model of Gas Release

To aid in developing an improved model for fission-gas release, an attempt is being made to evaluate microscopically the open and closed porosity of sintered UO_2 bodies. Specific differences in pore distribution have been observed. These differences appear to be related to the sintering atmosphere and may have marked effects upon the available surface area of UO_2 bodies of identical density but prepared by various methods. Since fission-gas release would be expected to increase with surface area, attempts are being made to relate pore size, distribution, and density to the surface area measured by gas-adsorption methods.

During November, preliminary estimates were made of the ratio of true surface area to geometrical surface area for several specimens. In this first approximation, a number of assumptions were made: (1) the pore size was assumed to be constant, (2) the pore diameter was taken as the maximum observed in a metallographic section, and (3) the pores were assumed to have no direct connection to subsurface pores, nor would grain boundaries provide this path. With these assumptions, the ratio of true surface area (S_T) to the geometrical surface area (S_G) can be approximated from a pore count and pore-size distribution, obtained from a metallographic section. The as-polished specimens were used in this analysis because examination of the etched specimens revealed many etch pits which to not appear to be associated with original pores. The S_T/S_G ratios for several UO_2 bodies are given in Table F-10. These results

indicate that surface pores would increase the surface area by no more than a factor of 2 for bodies of 95 per cent density. Additional measurements are needed on lower density bodies before any relationship can be established between surface area and pore structure. Gas-adsorption measurements on specimens having similar as-polished surfaces will be made to determine whether the surface pores connect with subsurface porosity.

TABLE F-10. MICROSCOPIC ANALYSIS OF TRUE SURFACE AREA VERSUS GEOMETRICAL SURFACE AREA OF SINTERED UO_2

Density, per cent of theoretical		Pore Diameter, μ		Pores per	
Pycnometric	Lineal Analysis	Maximum	Average[a]	Square Micron	S_T/S_G Ratio
95[b]	95	3.7	1.5	3.7×10^{-2}	1.73
93[c]	95.6	1.5	0.9	11.5×10^{-2}	1.65
97[b]	96	3.6	1.3	3.7×10^{-2}	1.71
98[c]	97	0.71	0.36	10.3×10^{-2}	1.70

(a) The average pore diameters may be in error due to difficulty in measuring the smaller pores.
(b) Bodies prepared from UO_2 powders, as hydrogen reduced from UO_3, compacted, and sintered in hydrogen.
(c) Bodies prepared from ball-milled Davison UO_2 compacted and sintered in argon.

Four metallographic specimens and two thin sections of UO_2 were irradiated during the last period to give an estimated 1 a/o displacement by fission fragments. Examinations of these specimens by light and electron microscopy is in progress. The thin sections fractured and became less transparent during the irradiation. However, the cause of fracture has not been ascertained. It is possible that new specimens will be needed for this study. Perhaps the thickness of the specimens can be reduced from approximately 30 μ to 5 μ and thus transmit more light at higher burnups. Replicas have been made of the metallographic specimens for further study.

A second batch of UO_2 boules was received from Mallinckrodt Chemical Works for evaluation. The boules are approximately 1/2 in. in diameter and 3/4 in. long. These are made up of large friable crystals which fracture easily along the axis of the cylindrical boule. Metallographic and thin-section examination of these crystals has revealed a second phase or a substructure of voids which was not observed in an early shipment. Although the amount of this structure is limited, it may require careful selection of specimens for fission-gas-release studies. Other specimens will be examined during the next period.

Diffusion in UO_2

Assembly of the apparatus to study the release of fission gas from refractory fuel specimens in the BMI Radioisotope Laboratory during postirradiation heat treating has been completed. Early in December, diffusion studies will be initiated with irradiated uranium dioxide. The first run will be devoted to determining the capabilities of the scintillation counting system for continuously measuring fission-gas release. This run will be followed by a series of measurements of the release rates of fission gases from spheres and plates of single-crystal uranium dioxide at temperatures from 1000 to 1600 C.

The BET microweighing surface-area measurements on fused single-crystal UO_2 bodies have not been entirely consistent; consequently, additional effort is being made to resolve the uncertainties. It was reported previously that large differences have been observed between plate-type and spherical specimens. Two plates (nominal area of 1 cm^2) with surfaces polished to metallographic quality did not have an area sufficient for detection by the BET method. However, a sphere (nominal area of 0.5 cm^2) polished to 600-grit-abrasive surface quality appeared to have a surface area of approximately 100 cm^2. In order to determine if microscopic surface irregularities affect surface-area measurements, the same sphere was polished to metallographic surface quality for measurements of surface area.

Experimental studies of the fusion of UO_2 powder in a plasma-jet flame were continued with emphasis on increasing the efficiency of fusion and avoiding oxidation of the UO_2. Vacuum degassing of UO_2 powder prior to fusion did not prevent the formation of higher oxides of uranium. One run was made on powder which had been milled in methanol for 120 hr and vacuum degassed. Higher oxides of uranium were observed in the fused product. Discoloration of the plasma-generator electrodes indicated that either air inleakage had occurred during the run or the gas-drying bed needed to be regenerated. The fraction of UO_2 fused remained relatively constant at about 80 per cent over the range of operating conditions studied. The bulk of the unfused material proved to be higher oxides of uranium. Future efforts will be directed at identifying and eliminating the source of oxygen contamination.

Preparation for In-Pile Study

A furnace and continuous sweep-gas system for in-pile heating of uranium dioxide specimens and for collection of released fission gases is under construction. The several components are an in-pile induction furnace designed for temperatures up to 3000 F, a fission-gas-collection system, using a nonrecirculating carrier gas, a carrier-gas-purification train, and supplementary equipment for continuous monitoring of the carrier gas-fission gas mixture and for intermittent analysis of the fission gas collected on activated charcoal.

The induction furnace has been assembled, and a program of out-of-pile furnace-heating tests is being conducted. Installation and initial check-out were completed on the 5-kw RF power unit. The furnace-heating characteristics were studied with the load coil-generator cirucit balanced to duplicate as near as possible the lead length anticipated for actual in-pile operation. Total time at temperature in excess of 2600 F for the specimen zone, including the power cycling, was approximately 2-1/2 hr. The total number of full power-no power cycles was approximately ten. In addition to this cycling, the generator power output was set at various levels for continuous operating intervals of about 30 min each. Optical-pyrometer temperature readings of the specimen zone indicated that the following power-temperature relations existed during this test:

F-27

Power Level at Generator Terminals, per cent of 5 kw	Range of Specimen-Zone Temperature Readings, F
25	1800 to 1900
50	2350 to 2450
65	2900 to 3000
100	>3600

The gas-purification system has been assembled and leak tested with satisfactory results. The fission-gas-trapping train has been installed in its California hood enclosure. Individual analytic fission-gas traps have been leak tested; leak testing of the assembled trapping train is still to be completed. The major tasks remaining in the completion of the fission-gas-trapping system include installation of the continuous monitoring scintillation crystal, photomultiplier tube, and gamma spectrometer, installation of the hood exhaust-air monitor, connection of the RF-generator coolant-water recirculator and temperature-control apparatus.

Preparation of sintered UO_2 specimens for possible study in-pile has continued. Three groups of 24 specimens each were prepared from Davison UO_2 powder for irradiation testing. Data on processing conditions, oxygen-to-uranium ratio, sintered density, and porosity are given in Table F-11. Spectrochemical analyses of a specimen from each group are given in Table F-12. Microscopic examination of polished sections of a specimen chosen from each group revealed little variation in the microstructure of a given pellet from top to bottom or from center to edge. The microstructure of Specimen 59 contained isolated areas of high intragranular porosity, while Specimens 57 and 58 were quite uniform. Most of the porosity in Specimen 57 was within grains, while most of the porosity in Specimen 58 was at grain boundaries.

Investigation of the effect of preoxidation temperature on properties of ceramics made from Davison UO_2 powder was continued. The powder was ball milled dry for 15 hr and then was oxidized for 2 hr at various temperatures. Specimens were pressed at 40,000 psi and sintered in hydrogen for 1 hr at 3000 F. Sintered densities were as follows:

Oxidation Temperature, F	Sintered Density, per cent of theoretical
Unoxidized	95
400	95
932	97
1200	97
1500	96

The effect of preoxidation on microstructure and oxygen-to-uranium ratio is being investigated.

TABLE F-11. PROCESSING CONDITIONS[a] AND SINTERED DENSITY AND POROSITY OF UO_2 IRRADIATION SPECIMENS

Specimen	Milling Time, hr	Forming Pressure, psi	Sintering Temperature, F	Sintered Density		Open Porosity, per cent	Closed Porosity, per cent	Oxygen-to-Uranium Ratio
				G per Cm^3	Per Cent of Theoretical			
57	15	40,000	2800	10.50	95.8	0.0	4.2	2.00
58	15	40,000	3000	9.42	85.9	0.1	14.0	2.08[b]
59	2	40,000	2800	10.02	91.0	1.5	7.5	2.00

(a) Specimens 57 and 59 were milled dry in a natural-rubber-lined mill with Borundum balls; Specimen 58 was milled similarly except in methanol. Sintering was done in flowing hydrogen on a schedule requiring about 6 hr to reach peak temperatures and a 1-hr soak at peak temperature.
(b) A duplicate specimen had an oxygen-to-uranium ratio of 2.10.

TABLE F-12. SPECTROCHEMICAL ANALYSES OF UO^2 IRRADIATION SPECIMENS

Specimen	Impurities Present, ppm												
	Si	Mn	Mg	Pb	Cr	Sn	Fe	Ni	Be	Mo	Cu	Ca	Al
57	20	1	5	4	30	7	60	100	<1	2	10	4	20
58	30	2	20	<1	<2	7	80	60	2	2	10	40	20
59	40	2	10	4	40	3	60	100	<1	10	5	20	40

F-29

GENERAL FUEL-ELEMENT DEVELOPMENT

S. J. Paprocki

Fabrication techniques are being developed for the preparation of cermet fuel materials containing 60 to 90 volume per cent of UO_2 dispersed in chromium, molybdenum, niobium, and stainless steel matrices. These materials have been prepared by cold pressing and sintering, hot-press forging, warm swaging, and gas-pressure bonding. When properly fabricated, cermets containing 80 volume per cent UO_2 possess a thermal conductivity three to six times better than bulk high-density UO_2.

The solid-phase bonding of molybdenum and niobium is being achieved by use of the gas-pressure-bonding process. Techniques for surface preparation and the bonding parameters of time, temperature, and pressure have been established for niobium. Flat-plate niobium-clad compartmented UO_2 fuel plates have been bonded. The individual compartments containing UO_2 were gas-pressure tested to rupture. The ruptures occurred through the cladding with considerable deflection, indicating good bond integrity and cladding ductility.

A fundamental study of the mechanism and kinetics of solid-phase bonding achieved by use of pressure at temperature is being investigated. The results from this study have direct practical application to the gas-pressure-bonding process.

Fabrication of Cermet Fuel Elements

S. J. Paprocki, D. L. Keller, G. W. Cunningham, and D. E. Kizer

Cermet fuel materials consisting of 60 to 90 volume per cent UO_2 dispersed in chromium, molybdenum, niobium, or stainless steel matrices have been investigated. Methods investigated for fabricating these materials to 90 per cent of theoretical density or better are hot press forging, warm swaging, and gas-pressure bonding of green-pressed pellets. Considerable cracking and directionality has been encountered with the hot-press-forging techniques. Warm swaging of the cermet cores has resulted in little or no densification; therefore, major emphasis is now being placed on fabricating cermets by gas-pressure-bonding techniques.

Thermal-conductivity measurements have been made on several cermet rods prepared by gas-pressure bonding with values ranging from three to six times that of reported bulk UO_2 values. Since spherical UO_2 powder has been found to enhance the microstructure of the cermets, additional cermet rods are being prepared for thermal-conductivity measurements using spherical UO_2 instead of high-fired UO_2 powder. In addition, it is planned to measure the conductivity of cermets prepared from metal-coated UO_2 powder for comparison with measured values of cermets prepared by mixing uncoated UO_2 powder and metal powder.

Several 80 volume per cent UO_2-molybdenum, niobium, or stainless steel green-pressed cermets have been prepared in rectangular shapes for pressure bonding to high

densities. These specimens will be used to determine modulus of rupture and thermal-shock resistance. Some delay has been encountered because of failure of cans in the welds during pressure bonding. Additional cermet cores will be pressure bonded in stainless steel cans instead of the Ti-Namel cans previously used.

A series of electrical-resistivity measurements have been made on an 80 volume per cent UO_2-molybdenum cermet rod of 91.1 per cent of theoretical density. Values of 2.0, 2.8, and 4.6×10^{-4} ohm-cm were measured, respectively, at 100, 300, and 600 C. Measurements were made simultaneously with thermal-conductivity measurements previously reported.

Investigations are being made to determine the feasibility of slip casting cermets to densities sufficiently high for pressure bonding. Slips cores have considerably higher green strength than those prepared by conventional powder-compacting techniques. Cermet containing slips are being prepared to study the effects of variation of pH and water content upon the casting.

Gas-Pressure Bonding of Molybdenum- and Niobium-Clad Fuel Elements

S. J. Paprocki, E. S. Hodge, and P. J. Gripshover

The gas-pressure-bonding technique is being investigated as a possible method for fabricating molybdenum- and niobium-clad ceramic and cermet-type fuels. The high-temperature strength and favorable nuclear properties of molybdenum and niobium make them promising structural materials for use in high-temperature inert-gas-cooled and some liquid-metal-cooled reactors.

Two additional niobium-clad compartmentalized flat-plate fuel elements have been pressure bonded at 2100 F and 10,000 psi for 3 hr. Each plate contained three outgassed UO_2-Al_2O_3 cores separated by 1/4-in.-wide strips of niobium. Graphite-coated Ti-Namel spacers were used to separate the bonding container from the fuel plates during gas-pressure bonding. Removal of the specimens from the bonding container was accomplished by pickling the graphite-coated Ti-Namel spacers away from the specimens in a solution of 1 part nitric acid and 1 part water. Visual examination of these elements indicated that excellent flow had occurred during bonding; however, there was some evidence of cracking of the cladding over several of the core compartments. Sections of the cladding taken from these areas do not indicate excessive brittleness; bend tests made in areas away from the cores showed excellent ductility. It appears that the core may be the cause of the unusual behavior of the cladding. Chemical analyses will be run to determine if any change in chemical composition occurred during bonding. It is also planned to bond a specimen containing pure UO_2 cores to determine if the Al_2O_3 that is present in the cores now being used caused the embrittlement of the cladding over the core areas.

Burst tests have been conducted on one of the two fuel elements described above. This test was accomplished by drilling a small hole through the cladding on one side of of a core and internally pressurizing through this hole until a cladding failure occurred.

The bursting pressure and deflection of the cladding at the time of failure were measured. Two compartments in the fuel element were burst tested; the first compartment burst at 2500 psi with a 54-mil deflection, while the second burst at 1500 psi with a 64-mil deflection. The reason for the difference in bursting pressure in the second compartment is attributed to local thinning of the cladding. It is significant to note that failure occurred through the cladding and not through the bond between the compartments, and the cladding deflected a large amount prior to failure. This indicates that the cladding was ductile after bonding and that the bonds were strong.

Studies to determine the optimum surface preparation for the self-bonding of molybdenum have been continued. Specimens have been prepared embodying plates of molybdenum which had been pickled in a solution of 2 parts nitric acid and 1 part water or 3 parts nitric acid and 1 part water. Examination of these specimens revealed that very little grain growth occurred across the original bond interfaces. However, there was very little contamination present along the interfaces, especially in the specimens pickled in the solution of 3 parts nitric acid and 1 part water. Since recrystallization was not complete in these specimens, it is felt that these experiments should be repeated with material which is more severely cold worked prior to bonding.

Several molybdenum specimens were pressure bonded to determine the effectiveness of chromium and graphite as barrier layers to prevent reaction between the molybdenum and the coated spacers. Specimens containing graphite-coated Ti-Namel showed slight evidence of reaction in some areas. This reaction is attributed to the graphite diffusion into the Ti-Namel during the bonding cycle, thereby exposing the Ti-Namel to the molybdenum. A specimen containing graphite-coated molybdenum spacers showed no evidence that the graphite had diffused into either the spacer or the molybdenum specimen, indicating that graphite may be a suitable barrier material.

A flat-plate molybdenum specimen pressure bonded at 2300 F and 10,000 psi for 3 hr containing chromium-coated Ti-Namel spacers showed very little reaction between the molybdenum and the chromium. This reaction zone could be easily removed by pickling in diluted nitric acid. Bend tests made on this specimen indicated that it had retained a large portion of its prebonding ductility. Chromium will be further investigated as a barrier material.

Factors Affecting Pressure Bonding

G. W. Cunningham and J. W. Spretnak

A study is being made of the mechanism and kinetics of solid-phase bonding under application of heat and pressure. The majority of the work at present is being conducted with OFHC copper specimens.

Hot-pressing equipment is being modified and the Chromel windings presently used are being replaced with molybdenum windings so as to permit hot pressing at temperatures to 2500 F. Graphite dies are available for the very high temperatures, and Stellite dies have recently been completed for use at intermediate temperatures. High-speed tool steel dies are used at temperatures below 1100 F.

F-32

Hot-pressing experiments have been interrupted while the equipment is being modified, but several annealing studies are in progress. A series of specimens pressed at 1000 C for 5 min at pressures ranging from 2,000 to 12,000 psi and previously evaluated in the as-pressed condition has been annealed at 1800 F for 24 hr in hydrogen. These specimens have not been evaluated, but they should provide information on the effect of distance along the bond interface to a free surface on grain growth across the interface. Also, unbonded specimens have been annealed in vacuo at 1800 F to provide samples with large grains to be used in studies on the effect of grain orientation at the interface on bonding characteristics and grain growth. Upon completion of modifications to the hot-press equipment, the studies of the effect of pressure on producing an interface in which the two surfaces are in intimate contact, the study of grain-orientation effects, and the study of factors discussed in previous reports will be resumed.

FF-1

FF. FUEL-CYCLE PROGRAM STUDIES

GAS-PRESSURE BONDING OF CERAMIC, CERMET, AND DISPERSION FUEL ELEMENTS

S. J. Paprocki, S. W. Porembka, D. L. Keller, E. S. Hodge,
C. B. Boyer, and J. B. Fox

This development program is concerned with the application of a fabrication process which will maintain or improve fuel-element quality and reduce manufacturing costs. The gas-pressure-bonding technique is being explored, as it appears to be a promising fabrication method for achieving these objectives. The ceramic, cermet, and dispersion fuel systems were selected because it is believed that these fuel systems offer the greatest potential for achieving a high burnup over a range of temperatures. They offer an excellent opportunity for a substantial cost reduction by the utilization of pressure bonding and also offer the possibility of improved performance. The study is directed toward the refinement and further development of the gas-pressure-bonding process to accomplish simultaneous densification and cladding of these fuels with stainless steel. The major emphasis is being placed on the development of fuel elements consisting of UO_2 ceramic bodies clad with Type 304 stainless steel. It is anticipated that this technique can also be utilized for uranium dioxide dispersion and cermet fuel systems with a minimum of development work.

Uranium Dioxide Compaction Studies

The studies to date have been concerned with the development of high-density green UO_2 cores of specific densities which will achieve a desired range of densities upon pressure bonding. Previous studies involved the cold-compacting characteristics of seven powder types and several powder mixtures. More recent efforts have been directed toward cold-compaction methods other than cold pressing.

Tap densities of various powder mixtures were measured in an effort to produce high-density UO_2 bodies without cold pressing. A mixture of 75 w/o MCW special dense UO_2 (minus 20 plus 325 mesh) and 25 w/o MCW ceramic grade UO_2 (minus 325 mesh) exhibited a tap density 59.1 per cent of theoretical (6.47 g per cm^3). Mixtures of 75 w/o Spencer fused UO_2 (minus 20 mesh) with 25 w/o MCW ceramic grade UO_2 (minus 325 mesh) and 25 w/o MCW high-fired grade UO_2 (minus 400 mesh) yielded densities of 57.1 and 68.0 per cent of theoretical, respectively (6.25 and 7.44 g per cm^3). The tap densities attained with these mixtures are not considered sufficient to minimize deformation of the stainless steel cladding during pressure bonding. Additional mixtures will be investigated.

Centrifuging of powders as a possible means of low-cost densification of powders and as a means to facilitate loading of tubular-type elements was briefly evaluated. Seven types and grades of commercial UO_2 were tested. These powders included MCW ceramic grade UO_2, MCW dense ceramic grade UO_2, MCW high-fired UO_2, MCW

special dense grade UO_2, MCW spherical grade UO_2, NUMEC high-fired grade UO_2, and a Spencer fused grade UO_2. Three mixtures were also tested. These mixtures were:

(1) 75 w/o MCW special dense UO_2 (minus 20 plus 325 mesh) and 25 w/o MCW ceramic grade UO_2 (minus 325 mesh)

(2) 75 w/o Spencer fused UO_2 (minus 20 plus 325 mesh) and 25 w/o MCW ceramic grade UO_2 (minus 325 mesh)

(3) 75 w/o Spencer fused UO_2 (minus 30 plus 325 mesh) and 25 w/o MCW high-fired UO_2 (minus 400 mesh).

Of the seven powder types and three powder mixtures, only the mixture of 75 w/o Spencer fused UO_2 and 25 w/o MCW high-fired UO_2 exhibited a good density. The density achieved in this case was 68 per cent of theoretical (7.43 g per cm^3), which is comparable to the tap density achieved in previous studies of the same powder mixture. Within the range of powders tested, no advantage of centrifuging was noted. It appears that powder-bridging effects prevented the attainment of high-packed densities.

Additional areas of work considered in the UO_2 compaction study include tap packing various mixtures, presintering to provide higher densities and to facilitate fuel-element loading, a study of the densification characteristics of various size fractions, and vibratory compaction.

Gas-Pressure Bonding

Previous gas-pressure-bonding studies have concerned the densification characteristics of various UO_2 powders during pressure bonding at 1900 to 2000 F. During the course of the pressure-bonding studies, internal spacer supports have been incorporated in bonded rod elements. More recent work has been concentrated on the evaluation of the stainless-stainless bonds, utilization of fuel-element designs which will provide for the high UO_2 densification experienced in previous tests, and a more complete evaluation of gas-pressure-bonded UO_2.

The effect of different surface preparations on the quality of Type 304 stainless steel bonds resulting from pressure bonding is being investigated. Flat-plate-specimen packs containing sheets 10, 20, and 75 mils thick, with each specimen pack representing as-rolled, belt-abraded, or vacuum-annealed surfaces have been prepared thus far. These were gas-pressure bonded for periods of 3 hr at 2000 and 2100 F at 10,000 psi. The specimens were evaluated by metallographic observation, along with peel and bend tests, as reported in Table FF-1.

Various element designs are being considered to minimize densification effects, warpage, and dimensional nonuniformity which occurs when pressure bonding tapped powders or cores of a low density. Three of these designs have been pressure bonded and show promise of being suitable for use as fuel elements. These include corrugated rod, corrugated plate, and a rib-supported rod. Other specimens of these designs are being prepared.

TABLE FF-1. EVALUATION OF SURFACE PREPARATION ON THE QUALITY OF TYPE 304 STAINLESS STEEL PRESSURE-BONDED BONDS

Surface Type	Surface Preparation of Components	Gas-Pressure-Bonding Conditions			Evaluation Comments
		Time, hr	Temperature, F	Pressure, psi	
As rolled	Degreased in alcohol and rinsed in cold water, 2-min pickle in an aqueous solution of 10 parts nitric acid heated to 120 F followed by cold-water rinse, detergent washes and hot-water rinses, and then air dried	3	2000	10,000	Bonds did not fail during bend and peel tests; metallographic examination revealed only a 25 per cent grain growth across the interface
		3	2100	10,000	Bonds did not fail during bend and peel tests; metallographic examination revealed 70 to 80 per cent grain growth across the interface
Belt abraded	Surfaces belt abraded with a 60-grit SiC abrasive belt to a surface finish of 20 to 25 μin. and then degreased, pickled, washed, and rinsed as the as-rolled specimens	3	2000	10,000	Bonds did not fail during bend and peel tests; metallographic examination revealed slight contamination and 25 to 30 per cent grain growth across the interface
		3	2100	10,000	Bonds withstood the bend and peel tests; metallographic examination revealed slight contamination and 95 per cent grain growth across the interface
Vacuum annealed	Components degreased in alcohol and rinsed in cold water and then vacuum annealed at 2100 F for 1 hr; no further treatment given the surface	3	2000	10,000	Bonds did not fracture during bend and peel tests; metallographic examination revealed slight contamination and only a 10 per cent grain growth across the bond interface
		3	2100	10,000	Bonds withstood the bend and peel tests; metallographic examination revealed 60 to 70 per cent grain growth across the bond interface

FF-4

Rod specimens containing different types of UO_2 are being prepared for pressure bonding to check the effect of pressure bonding upon the stoichiometry of the UO_2, the internal deforming pressures on the bonded rods, and the permeability of the UO_2 cores from the bonded rods.

DEVELOPMENT OF URANIUM CARBIDE-TYPE FUEL MATERIALS

F. A. Rough and W. Chubb

As a portion of the Fuel-Cycle Development Program sponsored by the AEC, an integrated program of research on the preparation and properties of uranium carbides is in progress at Battelle. This program involves investigations of the chemical preparation and forming of uranium carbides by powder metallurgy and by arc-melting and -casting techniques. In addition, the physical, mechanical, and corrosion properties of uranium carbides are being measured, and fundamental studies of diffusion rates in uranium carbides and of the nature of irradiation damage to carbides are being made.

A report summarizing the physical- and mechanical-property data obtained during the first 6 months of this research program was recently issued (BMI-1370). Since this report was completed, data have been reported in the monthly reports on the skull-casting process for making 2-in.-diameter castings of 100 per cent dense uranium carbide, on the final results of a study of interdiffusion rates in the UC-UC_2 system, on the corrosion rates of carbides in water and glycol and Santowax R, and on the compatibility of uranium monocarbide with Inconel, steel, stainless steel, aluminum, copper, molybdenum, and tantalum.

Current research has produced results which indicate that uranium monocarbide does not react with magnesium metal in 24 hr at 600 C. Uranium monocarbide reacts with zirconium metal at 1000 C, producing a zirconium-uranium solid solution on the surface of the zirconium in contact with the carbide. The rate of reaction was not catastrophic.

Tests of the compatibility of uranium monocarbide with NaK for 1 month at 1500 F (816 C) resulted in small weight losses. Since several of the specimens containing impurity additions disintegrated, and since these same impurity additions are known to produce cracks in castings, it is suggested that the measured weight losses were the result of spalling produced or accentuated by the presence of cracks in the specimens before testing.

Alternate Fabrication Methods for UC

S. J. Paprocki, D. E. Kizer, and J. M. Fackelmann

The objectives of this program are (1) to evaluate various methods of preparing UC powder, (2) determine the conditions required to sinter dense UC bodies from UC powder, and (3) investigate alternate methods of preparing dense UC bodies by

powder-metallurgy techniques such as the reaction of uranium and carbon powders. The comparative economics of the various alternatives will be considered with respect to ultimately preparing dense UC bodies.

Uranium metal was reacted with propane gas in anticipation of forming UC powder. The uranium was first hydrided to form a fine uranium powder prior to the addition of a 200-mm pressure of propane to the evacuated reaction chamber. The temperature was gradually increased through the range of 480 to 540 C, where an increase of pressure was noted on the hydrometer. When no further pressure increase was noted on heating with propane or cooling with hydrogen, the reaction was considered complete. The resulting powder was extremely fine and black in color. A chemical analysis showed a total carbon content of 3.76 w/o and a free-carbon content of 0.20 w/o. Additional studies are being made with the uranium-propane reaction, which has been noted to be more rapid than the uranium-methane reaction.

Studies have continued on the sintering of arc-melted and crushed UC powder. The results of recent experiments are shown in Table FF-2. In each case the green density was approximately 60 per cent of theoretical. This was obtained by pressing the wax-coated UC powder (minus 325 mesh) at approximately 13 tsi.

TABLE FF-2. SINTERING DATA FOR UC COMPACTS PREPARED FROM ARC-MELTED MINUS 325-MESH POWDER

Sintering Conditions		Sintered Density[a],
Time, min	Temperature, C	per cent theoretical
5	1840	70.2
5	1840	71.5
35	1840	75.2
35	1840	67.3
10	1840	74.5

(a) Green density was approximately 60 per cent of theoretical after pressing at about 13 tsi.

It is apparent from these preliminary data that a sintered density of 90 per cent or greater cannot be obtained with the particular powder investigated unless excessively high sintering temperatures (greater than 2000 C) are used. Particular attention, therefore, will be given to possible methods of accelerating the densification process. Among the methods to be studied are (1) use of decreased particle size, which increases particle contacts per unit volume, (2) application of an external load during sintering, and (3) use of carbon-rich and carbon-deficient structures, which may lead to increased sinterability.

With respect to forming UC bodies by the reaction of uranium and carbon, a mixture of 4.8 w/o Norite-A activated charcoal and minus 325-mesh uranium powder was

hot pressed at 800 C for 15 min under a pressure of 12 tsi to a density of 9.10 g per cm^3. The core was transferred to a high-vacuum furnace and heated at 1050 C for 4 hr prior to rapid heating to 1760 C, where core melting was not observed. A microscopic examination indicated a structure of UC with alpha uranium at the grain boundaries and along the edges. The presence of alpha uranium may be due to decarburization during the various heat treatments.

Melting and Casting Techniques for Uranium-Carbon Alloys

B. L. Boesser, W. M. Phillips, E. L. Foster, and R. F. Dickerson

Uranium carbide is a promising nuclear fuel because of its high melting point, uranium density, and thermal conductivity. Reliable techniques for the production of high-quality cast shapes of uranium carbide are being developed.

During the past month, castings of various cross sections up to 4 sq. in. in area and 8 in. long have been made in the skull-type arc furnace. Although large cast shapes of good quality, in terms of soundness and surface condition, can be produced in the skull-type arc furnace, the composition control effected has not been satisfactory. Appreciable carbon pickup by the molten uranium carbide from the graphite crucible liner and the graphite electrode tip is possible; in some instances a casting containing about 6 w/o carbon is produced from a starting charge containing less than 2 w/o carbon. It has been established that the major portion of this excess carbon comes from the graphite-crucible liner that is used during melting. Consequently, the crucible liner has been replaced by a UC skull which is in direct contact with the water-cooled copper crucible.

A series of castings will be made to determine if a correlation exists between electrode losses and the carbon picked up by the melt, and also to establish reliable techniques for control of composition using a melting hearth consisting entirely of a uranium carbide skull. Future work will also include efforts to develop castings with good surface quality and better internal soundness and structure. Molds for multiple castings will be made and used in attempts to produce several castings with one pouring. A study of the feasibility of different methods for melting and casting uranium carbide will also be made in the future.

Metallurgical and Engineering Properties of Uranium Monocarbide

W. M. Phillips, E. L. Foster, and R. F. Dickerson

The present study of uranium monocarbide is concerned with the definition and improvement of the properties of this material. Such variables as impurity content, carbon content, and heat treatment are being evaluated on the basis of their effect on density, rupture strength, electrical resistivity, thermal conductivity, and corrosion resistance.

FF-7

Corrosion resistance and compatibility with possible cladding materials were investigated during the past month. Compatibility tests of uranium monocarbide in contact with zirconium at 1000 and 1200 C for 24 hr produced extensive reaction zones between the two materials. The products of the reaction are believed to be zirconium-uranium carbide and a uranium-zirconium solid solution. Similar tests in which magnesium was placed in contact with uranium monocarbide at 600 C for 24 hr produced no observable reaction.

Corrosion testing of uranium monocarbide in commercial NaK at 1500 F for 1 month produced small weight changes in the specimens. Most of the losses are believed to be the result of mechanical chipping of the specimen corners during handling and testing. Several of the specimens containing 800 ppm iron or silicon or 10 ppm hydrogen disintegrated during testing. The effect is attributed to cracking, produced by the additions, in the original casting. The balance of the specimens containing up to 800 ppm nitrogen, oxygen, or tungsten or no impurities showed only a slight etching-type of attack.

Residual stresses in cast specimens are being investigated by varying the heat-treating temperatures and the amount of surface removed by grinding. Corrosion testing of binary carbides is also in progress.

Uranium Monocarbide Diffusion Studies

W. Chubb, R. W. Getz, and F. A. Rough

The rate of self-diffusion of uranium in uranium monocarbide is being studied using a tracer technique. The study of diffusion rates in uranium monocarbide is of interest because this material is being considered as a possible reactor fuel for high-temperature operation. Currently, diffusion couples are being prepared using uranium monocarbide made with depleted uranium (0.04 per cent uranium-235) and 0.001-in.-thick foil of enriched uranium metal (93 per cent uranium-235).

The necessary physical and mechanical techniques for studying the rate of self-diffusion of uranium in uranium monocarbide are being perfected. Depleted uranium was used in making castings of uranium monocarbide 0.50 in. in diameter. These cylindrical castings were cut into 0.25-in.-lengths using a diamond cut-off wheel and kerosene coolant. An enriched uranium foil is to be placed between two lengths of the monocarbide to form a diffusion couple. The couple will be wrapped in tantalum foil and inserted in a graphite jig for pressure bonding and annealing in vacuum. This procedure reduces the contamination of the bond by graphite and oxygen. A couple, containing normal uranium components, has been bonded by heating for 4 hr at 1400 C followed by 1 hr at 1800 C. This couple was examined metallographically and appeared to be well bonded. It is planned to prepare diffusion couples that have been subjected to temperatures between 1600 and 2000 C for a minimum period of 1 hr.

After annealing, the diffusion couples will be mounted in Bakelite, and analytical samples will be obtained by grinding the couple with 600-grit silicon carbide powder and simultaneously dissolving the uranium carbide in a nitric acid solution. The grinding will be done in a flat-bottomed aluminum dish, since the silicon carbide stone previously

selected for this operation was found to load with uranium during grinding. Analytical samples were obtained using the aluminum dish and are being analyzed for uranium content. These samples were prepared to determine if all the uranium ground from a measured length of uranium carbide is recovered in the nitric acid solution.

The grinding technique just described will be used to prepare samples for activation in the BRR. Gamma counting of the fission products from uranium-235 will be done to determine the amount of uranium-235 present in the sample. From these data it will be possible to calculate the rate of self-diffusion of uranium in uranium monocarbide. All preliminary activations and calculations have been completed.

Future work will include further evaluation of the bonding and sampling techniques being used, and the preparation of additional diffusion couples made from depleted uranium monocarbide rods and enriched uranium-metal foil.

Irradiation Effects in UC

A. E. Austin and C. M. Schwartz

The effect of irradiation on structural properties of UC is being studied. Equipment has been constructed for preparing radioactive powder samples for X-ray diffraction and is being tried with unirradiated material. The equipment provides means for crushing, sieving, and mounting powder in plastic holders under a protective argon atmosphere.

Electron-microscope examination of previously irradiated specimens with estimated burnups of 0.05 and 0.2 a/o is in progress. The macro replicas were made in a dry atmosphere by wetting the specimen with methyl acetate, pressing a sheet of cellulose acetate against the wet surface, and drying. The macro replicas are used for preparation of final replicas for electron microscopy by conventional techniques. This method used with unirradiated UC gave replicas without artifacts of either bubbles or local pitting from reaction with moisture.

GG-1 and GG-2

GG. VOID-DISTRIBUTION AND HEAT-TRANSFER STUDIES

D. V. Grillot, R. Wooten, H. M. Epstein, and J. W. Chastain

During November, check-out and preliminary operation of the loop continued. A great deal of difficulty was encountered in sealing around pressure taps in the 10-mil wall of the test section and in preventing short circuits between the test section and the backup housing when pressure is applied. Better silver soldering and support techniques were developed to solve the first problem, and transite insulation was substituted for the Durablac to solve the second.

Low-power runs were initiated. Void-distribution, heat-transfer, and pressure-drop tests will continue through the next month.

An ionization chamber, designed for high beta response and low gamma sensitivity has been completed. It will be tested with a mock test section to determine if it is more accurate and stable than the Geiger counter now in use.

H-1

H. PHYSICAL RESEARCH

F. A. Rough

In the study of the mechanism of migration of hydrogen in zirconium hydride, successful procedures have been developed for pressure bonding the necessary hydride-containing samples for a series of migration experiments. Also, diffusion coefficients of hydrogen in the delta hydride have been obtained by two methods, and the results are in agreement.

Initial experiments to determine the feasibility of preparation of UO_2 single crystals by a vapor-deposition process and by fusion methods have been performed.

Thermal Migration of Hydrogen in Zirconium

J. W. Droege, W. M. Albrecht,
W. D. Goode, and H. H. Krause

The migration of hydrogen in zirconium under the influence of a thermal gradient is being examined. Improved pressure-bonding techniques have resulted in successful fabrication of a diffusion cell with suitable bonding of the zirconium hydride to the stainless steel container. The values of the diffusion coefficients for hydrogen in delta zirconium hydride obtained by two different methods are in good agreement.

Thermal Diffusion

Because of the problems encountered in the bonding of the zirconium hydride to the stainless steel container of the diffusion cell, a test element of new design was assembled. The size of the zirconium hydride disk was increased to 1/2 in. in thickness and 1 in. in diameter. A 1-in. thickness of Armco iron was substituted for the thin sheet of stainless steel previously used to separate the copper cylinders from the zirconium hydride.

Pressure bonding was accomplished by applying 10,000 psi of helium pressure at 1800 F for 2 hrs, followed by 1 hr at 1900 F. The element was then sectioned and examined metallographically. It was found that the pressure-bonding technique had resulted in good metallurgical bond formation between the stainless steel jacket and the zirconium hydride. This bonding procedure is being used to fabricate the thermal-diffusion cell for installation in the thermal-gradient furnace.

The pressure-measuring apparatus has been modified by the addition of a differential manometer, and two Pirani elements have also been added to the system. The furnace is to be controlled in such a way as to match the thermal gradient in the diffusion cell, which is established by means of heating and cooling coils wrapped around the ends of the cell.

H-2

A complete diffusion cell of the improved design is now being fabricated, and when calibrations are completed, the thermal-diffusion coefficient will be determined from a measurement of the temperature and the hydrogen pressure at each face of the zirconium hydride disk.

Diffusion Coefficients

The apparatus and procedures for determining the permeation rate of hydrogen through zirconium hydride were altered to provide adequate control of equilibrium-hydrogen pressures up to 1 atm. The pressure regulator on the downstream side of the permeation cell was removed, and the downstream volume of the cell was isolated. The permeation rate was determined by measuring the increase in pressure on the downstream side of the cell with time.

The diffusion coefficients for hydrogen in zirconium hydride were determined by both the steady-state and time-lag methods. The equation for steady-state permeation is

$$F = \Delta Q / \Delta t = A/\ell \, D \, (C_1 - C_2), \qquad \text{(H-1)}$$

where

F = permeation rate

Q = quantity of gas that has permeated the disk in time t t

A = area of one face of the disk

ℓ = thickness of the disk

C_1 and C_2 = the respective equilibrium concentrations on the upstream and downstream faces of the disk determined by the respective pressures, p_1 and p_2, and temperature of the sample

D = diffusion coefficient.

Integration equation (H-1) gives

$$Q = A/\ell \, D \, (C_1 - C_2) \, t + \text{constant}. \qquad \text{(H-2)}$$

For relatively small differences in C_1 and C_2, a linear pressure relationship can be used to give the approximation

$$C_1 - C_2 \simeq \Delta \, c/\Delta \, p \, (p_1 - p_2). \qquad \text{(H-3)}$$

Also, Q may be expressed as

$$Q = \Delta \, Q/\Delta \, p_2 \, (p_2 - p_a), \qquad \text{(H-4)}$$

H-3

where $p_a = p_2$ at $t = 0$. Substituting Equations (H-3) and (H-4) into Equation (H-2) yields the relationship

$$\frac{p_2 - p_a}{p_1 - p_2} = \frac{\Delta c/\Delta p}{\Delta Q/\Delta p_2} \frac{A}{\ell} D\, t + \text{constant.} \qquad \text{(H-5)}$$

Experimental data are plotted on a graph of $(p_2 - p_a) / (p_1 - p_2)$ versus time. A straight line (steady-state rate) is obtained after an initial period. From the slope of the line and the value of $\Delta Q/\Delta p_2$, the diffusion coefficient can be calculated using Equation (H-5). The intercept of the straight line on the time axis gives a value for the time lag, L.

Several experiments have been made to determine the diffusion coefficients for hydrogen in zirconium hydride in the range 500 to 750 C, using samples having an average concentration of 60 to 66 a/o hydrogen. The experimental pressures, p_1 and p_2, were chosen so that the difference in concentration between the two faces of the disk was less than 2 a/o. The value of $\Delta Q/\Delta p_2$ was determined by noting the pressure change when a known volume of gas was removed from the system.

The values of the diffusion coefficients obtained to date are given in Table H-1. It can be seen that there is good agreement between the two methods of determining D.

TABLE H-1. DIFFUSION COEFFICIENTS FOR HYDROGEN IN ZIRCONIUM HYDRIDE

Temperature, C	Average Composition, a/o hydrogen	Diffusion Coefficient, D, 10^{-6} cm^2 sec	
		Steady-State	Time-Lag
500	65.8	0.15	0.21
600	63.3	1.2	1.1
700	59.8	7.2	7.1
700	60.0	7.2	--
700	60.0	7.6	--
750	60.0	29	27

Further experiments are being made at different hydrogen concentrations (in the range 60 to 66 a/o) for the same temperatures. The results should indicate the effect of hydrogen concentration on the diffusion coefficient.

Growth of UO_2 Crystals From the Vapor Phase

C. A. Alexander and R. B. Filbert, Jr.

During the past month, experiments were begun in producing UO_2 crystals from the vapor phase. This first effort has been directed at producing UO_2 crystals by utilizing the high volatility of UO_3 as the vaporizing species. The reaction

H-4

$$UO_{2+x} + \frac{1-x}{2} O_2 \rightarrow UO_3(g),$$

where x varied from 0.62 to 0.20, has been employed in the investigation.

Runs have been performed both in high vacuum and in inert-gas environments. To date, the largest crystals produced (about 800μ) have been made in the vacuum runs. The procedure for such runs is to fill a platinum crucible with U_3O_8 and support a platinum target (maintained at a temperature slightly below that of the charge) above the crucible. This assembly is placed in a closed-end ceramic tube, and the charge is heated to the desired temperature. Temperature limitations of the ceramic tube restrict the maximum operating temperature to about 1470 C. Next, the tube is evacuated at temperature, whereupon the U_3O_8 charge begins to disproportionate to $UO_{2+x} + O_2$, thus providing the oxygen for the formation of the $UO_3(g)$ from the remaining charge. The gaseous UO_3 formed in this manner decomposes upon condensation on the target to the equilibrium oxide at the temperature and oxygen pressure present at the target. The necessity for maintaining the oxide in the UO_2 phase region requires a high target temperature and low oxygen pressures or otherwise U_3O_8 will be produced.

Crystals have been formed on the surface of the charge as well as on the target. At the surface, supersaturation must be exceedingly small; hence it would appear that this crystal growth occurs through nucleation by dislocation. The target temperature has been varied from 10 to 40 C cooler than the charge with no appreciable effect upon the number or size of the crystals.

The experiment performed in the presence of the inert gas did not yield as many or as large crystals as did the vacuum runs. In this run, the charge of UO_2 was heated in pure argon to 1470 C, at which time argon with 0.3 volume per cent oxygen was passed over the charge to provide oxygen for the formation of $UO_3(g)$. This gas mixture was maintained in contact with the charge for 125 hr, at which time the system was purged with pure argon and cooled to room temperature in argon. Examination showed that a very few small crystals had formed on the charge surface and even fewer on the target. Three nested crucibles were employed in this run, so the bottom of one crucible formed the target for the one below it, but no significant differences in the size or number of crystals were found in the different crucibles. It is not too surprising that there were few crystals on the targets, due to the low mean free path, but it was surprising to find so few crystals on the surface of the charges where growth had been expected in this run. Two possible explanations for the limited number of crystals on the targets are (1) either the presence of the inert gas at the charge interface prevented crystal growth, or (2) the volatility of UO_3 is quite small if the U_3O_8 phase is absent. The amount of oxygen in the gas stream was selected so that the UO_2 would be oxidized no higher than $UO_{2.2}$, and since no quantitative data exist for the vapor pressures of UO_3 over any oxide lower than the two-phase region of UO_{2+x}-U_3O_8, it cannot be determined from this experiment alone if the volatility was lower than the calculated value.

For the coming month, it is planned to further investigate crystal growth from $UO_3(g)$ and to consider other reactions yielding volatile uranium oxides.

H-5 and H-6

Fusion Methods to Prepare Single Crystals of UO_2

W. P. Allred and B. Paris

During the month of November, work was contined to determine the possibility of using either electron-beam melting or induction melting to grow single crystals of UO_2 by the floating-zone technique.

It has now been established that, due to the high vacuum necessary for electron-beam melting, the process is not feasible for zone melting presently available samples of UO_2. The vapor pressure of this UO_2 material at its melting point appears to be too high (greater than 5×10^{-2}mm of mercury), and the sample sublimes before complete melting occurs. It may be desirable to re-evaluate electron-beam melting for growth of single crystals with higher purity stoichiometric UO_2.

Results of experiments on growing single crystals of UO_2 using a high-frequency RF generator to melt the material are encouraging. Direct coupling to the UO_2 has been demonstrated. This was accomplished by first heating the UO_2 to above 1200 C by passing an a-c current of approximately 12 amp directly through the UO_2 rod. However, zone melting by use of the RF generator has not yet been accomplished. Problems such as high-resistance contacts between the UO_2 and the chucks, and arcing between the UO_2 and the work coil still must be solved. At the present time the contact resistance is reduced by use of silver paint. It is planned to use metallic uranium near the ends of the UO_2 sample to reduce the contact resistance. The metallic uranium will be pressed into the rod during fabrication.

Attempts to eliminate arcing between the work coil and the sample will be made by increasing the spacing between the coil and the work or by using mica as an insulator between the work and the coil.

Studies in December will be concentrated on development of the induction-melting method for recrystallization and crystal growth of UO_2.

I-1

I. SOLID HOMOGENEOUS FUELED REACTORS

W. S. Diethorn and W. H. Goldthwaite

In support of the Pebble-Bed Reactor program Battelle is studying the properties and fission-gas retention of fueled-graphite spheres supplied by commercial vendors.

LABORATORY EVALUATIONS OF FUELED-GRAPHITE SPHERES

J. F. Lynch, M. C. Brockway, S. Rubin,
W. C. Riley, and W. H. Duckworth

Behavior under impact and compression tests and the coating integrity of coated fueled-graphite spheres are being studied with specimens received from commercial vendors.

The load-deflection curves near zero load have been determined for a few selected spheres in compression tests.

In the self-welding study, two SiC-coated spheres of a different type than that reported last month (BMI-1391) were tested at 2500 F for 66 hr under a load of 50 lb. A helium atmosphere was maintained throughout the test. The test was stopped short of the scheduled 100 hr because of a thermocouple failure. The spheres welded to each other and to the graphite used to hold both specimens in the furnace.

Two trial runs were completed with two coated spheres in the high-temperature gas-permeability apparatus. Gas samples are being analyzed.

The first results from the study of coating integrity of spheres under high internal gas pressures are available after successful development of a method of sealing a pressure fitting to a coated-graphite sphere. The sphere was submerged in hot silicone oil (380 F) during this test at 300 psia. There was no evidence of coating leakage from this SiC-coated sphere.

EVALUATION OF METAL-COATED UO_2 PARTICLES

A. F. Gerds, J. Koretzky, and F. W. Boulger

Work on metal-coated particles has been terminated. Studies of the reaction between alumina-coated UO_2 and carbon are continuing. Metallographic results are not available from the current studies with this latter system.

I-2

FABRICATION DEVELOPMENT OF Al_2O_3-CLAD UO_2 FUEL PARTICLES

A. K. Smalley and W. H. Duckworth

Processing variables are being studied in a continuation of the work reported last month in BMI-1391.

Selected batches will be evaluated in high-temperature air-oxidation tests, and advanced to the neutron-activation phase of the program.

FISSION-PRODUCT RELEASE FROM FUELED-GRAPHITE SPHERES

W. S. Diethorn

Fueled-graphite spheres are being investigated in neutron-activation experiments and in sweep-gas and static irradiation capsules.

Neutron-Activation Studies

H. S. Rosenberg and D. N. Sunderman

There is nothing to report this month.

In-Pile Capsule Experiments

D. B. Hamilton, D. Stahl, G. E. Raines, R. J. Burian, and W. H. Goldthwaite

SP-3

With the exception of metallography, the postirradiation examination of fueled-graphite specimens in SP-3 was reported in the August monthly report (BMI-1377). This capsule contained two FA-6 and two FA-8 specimens, fueled with UC/UC_2, which were both coated with siliconized SiC, and supplied by different vendors. In the FA-6 sphere an unfueled graphite shell separates the coating from the fueled-graphite core of the sphere. Metallographic examination of one sphere of each type is nearly complete, and the results are reported below.

There is no visible effect of irradiation on the microstructure of either specimen. Small microcracks in graphite are difficult to detect, but there is good evidence that very few microcracks were produced in the graphite regions during irradiation. The

coating of the FA-6 specimen is also free of microcracks. Metallographic examination of the FA-8 coating has not been completed.

Photomicrographs of the fuel particles and the surrounding graphite region show no effects which are not associated with particles and graphite in unirradiated spheres of the same type.

In December, metallographic examination of the FA-8 coating will be continued.

SP-4

The static-capsule experiment in the BRR continues to operate satisfactorily.

SP-5 and SPH-1

There is nothing new to report.

SPF-1

This low-flux capsule experiment was described last month in BMI-1391. In Table I-1, all fission-gas results, including corrected values for the first five runs reported last month, are summarized for the month of October.

Comparison of the R/B values at the two different fluxes reveals no flux effect, although the spread in values for some of the species could obscure a small flux effect. All species do not exhibit the same uniformity of R/B over the operating period, the data for xenon-135 suggesting a flux effect. This change in R/B with flux for xenon-135 is not believed to be a true effect of flux.

The experiment was terminated on October 30 in preparation for unmanned operation in late November. Capsule startup is expected in early December. The capsule will be operated several days at 1000 F.

SPF-2

There is nothing to report on this capsule experiment.

TABLE I-1. SUMMARY OF SPF-1 DATA AT 1500 F

Gas Sample	Collection Date, 1959	Temperature, F	Flux, $n/(cm^2)(sec)$	R/B[b] Krypton-87	Krypton-88	Krypton-85m	Xenon-135	Xenon-133
1[a]	10-14	1500	3×10^{10}	1.2×10^{-2}	4.7×10^{-3}	3.6×10^{-2}	2.4×10^{-2}	1.4×10^{-1}
2	10-15	1500	3×10^{10}	1.4×10^{-2}	3.8×10^{-3}	5.4×10^{-2}	1.9×10^{-2}	1.7×10^{-2}
3	10-16	1500	3×10^{10}	1.2×10^{-2}	2.2×10^{-3}	1.6×10^{-2}	1.6×10^{-2}	4.0×10^{-2}
4	10-18	1500	3×10^{10}	(c)	(c)	3.3×10^{-2}	2.8×10^{-2}	2.6×10^{-2}
5	10-19	1500	3×10^{10}	1.2×10^{-2}	4.6×10^{-3}	8.6×10^{-2}	6.3×10^{-2}	3.9×10^{-2}
6	10-23	1500	4×10^{9}	1.1×10^{-2}	5.8×10^{-3}	1.5×10^{-2}	8.8×10^{-3}	5.5×10^{-2}
7	10-26	1500	4×10^{9}	1.6×10^{-2}	4.2×10^{-3}	1.7×10^{-2}	9.0×10^{-3}	3.7×10^{-2}
8	10-28	1500	4×10^{9}	1.2×10^{-2}	3.1×10^{-3}	1.6×10^{-2}	8.4×10^{-3}	4.0×10^{-2}
9	10-30	1500	4×10^{9}	1.2×10^{-2}	2.8×10^{-3}	1.6×10^{-2}	9.8×10^{-3}	3.3×10^{-2}

(a) Collected 9 hr after capsule startup.
(b) R = the number of atoms released per second from the sphere.
B = the number of atoms produced per second in the sphere.
(c) Delay between sample collection and analysis prevented assay.

J. PROBLEMS ASSOCIATED WITH THE RECOVERY OF SPENT REACTOR FUEL ELEMENTS

CORROSION STUDIES OF THE FLUORIDE-VOLATILITY PROCESS

P. D. Miller, C. L. Peterson, W. N. Stiegelmeyer, and F. W. Fink

Evaluations of the corrosion which has occurred on various articles of process equipment used at ORNL for studies of the Fluoride-Volatility process are under way as part of a program of assistance to the Chemical Technology Division.

The examination of components from the Unit Operations INOR-8 dissolver is almost completed. Previous reports have described the major findings. A recent analysis of the scale on the inner wall of the dissolver vessel and of the draft tube showed that some selective leaching of chromium and iron from the INOR-8 metal occurred during the corrosion process.

The corrosion examination has shown that the liquid-gas interface areas are the most severely attacked during hydrofluorination. The attack is largely in the form of pitting. The corrosion is markedly retarded as long as dissolving zirconium remains in the container.

The HF gas-inlet line and thermocouple tubes in the Unit Operations Mk-I copper-lined hydrofluorinator were also severely attacked at the interface area. These tubes were made from Inconel and were exposed for less than 500 hr. The thermocouple tubes, which had a wall thickness of about 35 mils, were severed. The attack was intergranular, but was visible only to the depth of about one grain.

STUDY OF THE EFFECTS OF IRRADIATION ON CLADDING- AND CORE-DISSOLUTION PROCESSES

R. A. Ewing, H. B. Brugger, and D. N. Sunderman

Sulfex Process

Dissolution experiments with irradiated 7-in. prototype Consolidated Edison fuel pins (irradiated at ORNL) have begun in the hot cell. One dissolution is completed; a second has been carried through the decladding stage.

Test HS-1 (Pin A-103)

The surface of Pin A-103 appeared, under a stereomicroscope, to be clean and bright. No passivation was observed when the pin was immersed in the boiling 6 M

H_2SO_4 decladding solution; attack was immediate and vigorous. Small intermediate samples were withdrawn after 3 and 4 hr; the balance of the decladding solution was withdrawn after 6 hr. Decladding appeared visually to be complete, except for the end caps. Prior to core dissolution one core pellet was removed for a density determination. The value obtained was 8.52 g per cm^3, approximately 87.5 per cent of theoretical.

The dissolver vessel failed about 1/2 hr after introduction of the core dissolvent, presumably the result of thermal shock. Approximately 18.9 g of undissolved material was recovered, of which 6.4 g was end-cap material. Most of the loss appeared to be due to dissolution; however, there was apparently also considerable fragmentation of some of the core pellets into pieces too small to recover. This fragmentation seems to be an irradiation effect; although observed in both tests of irradiated fuel pins, it was never observed in the preliminary tests of similar unirradiated prototype fuel pins.

Core dissolution was continued on the recovered material using the standard procedure except that the quantity of HNO_3 was reduced.

Test HS-2 (Pin A-117)

Under the stereomicroscope the surface of Pin A-117 appeared to be generally dull, noticeably less bright than Pin A-103. This pin was passive; there was no attack by boiling 6 M H_2SO_4 in 1 hr. After the addition of formic acid (to 0.1 M concentration) failed to break the passivation, the 6 M acid was withdrawn and replaced by 8 M H_2SO_4. This appeared to attack the cladding upon reaching the boiling point. The cladding solution was sampled after 3 hr and withdrawn after 6 hr, at which time it was discovered that passivation had recurred during decladding, so that the fuel pin was still whole. Decladding was continued the following day with fresh 8 M H_2SO_4. The pin was still passive; passivation was finally broken by touching it with a steel rod, after which attack was vigorous. This cladding solution, withdrawn after 3 hr, removed the balance of the cladding.

Core fragmentation was again observed in this test. Considerable difficulties were encountered with plugging of the capillary liquid-transfer lines during removal of the cladding and wash solutions by small fragments of core. After completion of washing, the cladding and core residue (42.2 g) was removed and the test suspended; it will be resumed in December, when hot-cell space will again be available.

These first two tests of irradiated fuel pins have disclosed a need for additional apparatus modification, not apparent in the preliminary tests of unirradiated pins. Most important is the need for larger diameter lines for liquid transfer. The first 2 weeks of December will be devoted to apparatus modification and to analysis of the samples from Tests HS-1 and HS-2. Hot-cell dissolution tests are scheduled for the balance of the month; it is expected that dissolution of the remaining four ORNL-irradiated pins can be completed during this period.

Darex Process

Two Darex dissolution tests will be run following the completion of the Sulfex runs. No work on the Darex process was done during November.

K-1

K. DEVELOPMENTS FOR SRE

EVALUATION OF URANIUM MONOCARBIDE AS A REACTOR FUEL

F. A. Rough

Hot-cell examination of two additional capsules of uranium monocarbide specimens has been partially completed for Atomics International with satisfactory results. One capsule of specimens was irradiated to an estimated 13,000 to 14,300 MWD/T uranium. Complete evaluation cannot be made, however, until additional details are completed. Two capsules of specimens are continuing to be irradiated, one of them to an intended burnup of 20,000 MWD/T uranium.

Preparation of a series of enriched uranium carbide specimens with both as-cast and machined surfaces has been completed. These specimens will be irradiated by Atomics International in the SRE.

Irradiation of Uranium Monocarbide

D. Stahl, J. H. Stang, and W. H. Goldthwaite

This program has involved the irradiation at the MTR of six capsules containing cylindrical specimens of UC maintained in the 1000 to 1500 F range during in-pile exposure. Two of these capsules, BMI-23-4 and BMI-23-6, are still being irradiated. In general, during the irradiations of BMI-23-6, specimen center-line temperatures have been in the 1300 to 1500 F range, while the corresponding levels for specimens in BMI-23-4 have been lower, in the 1000 to 1300 F range. During MTR Cycle 130, which spanned most of November, this situation continued; core temperatures in the case of BMI-23-6 ranged from 1400 to 1500 F, while those in BMI-23-4 averaged about 1150 F, with a maximum of about 1250 F. These levels, which are estimated from readings of a thermocouple adjacent to the top specimen in each capsule, are about 150 F higher than those maintained during Cycles 128 and 129; removal of neighboring experiments prior to Cycle 130 is believed to have resulted in an increased flux in the irradiation positions occupied.

Capsule BMI-23-6 will be discharged at the end of Cycle 131; it is estimated that the burnup at this time will reach 5000 MWD/T of uranium. Capsule BMI-23-4 was to have completed its irradiation at the end of Cycle 132 to a burnup of 15,000 MWD/T of uranium. However, the irradiation of this capsule has been extended to obtain a burnup of 20,000 MWD/T of uranium. A request has been submitted to MTR personnel to move this capsule to a higher flux position to produce specimen temperatures close to 1500 F. Pending such a move, the irradiation of BMI-23-4 will continue in the present position (A-27-SE).

K-2

Postirradiation Examination of Irradiated Uranium Monocarbide

S. Alfant, A. W. Hare, F. A. Rough, and R. F. Dickerson

A program to determine the effects of neutron irradiation on uranium monocarbide is in progress. The investigation includes the examination of UC specimens with nominal compositions of 4.6, 4.8, and 5.0 w/o carbon before and after irradiation.

To date, three capsules containing UC specimens with nominal compositions of 5.0 w/o carbon have been irradiated and examined. A comparison of preirradiation and postirradiation data on specimens irradiated in the MTR for times up to six cycles and involving estimated burnups of up to 5700 MWD/T of uranium, and with maximum fuel-core temperatures of up to 1830 F, revealed no severe effects on the dimensional stability of UC.

During November Capsules BMI-23-3 and BMI-23-5 were discharged from the MTR and returned to the BMI Hot-Cell Facility for postirradiation examination. Capsule BMI-23-3, containing UC specimens having a nominal carbon content of 5 w/o, was irradiated in Position A-28-NE for 12 cycles with uranium burnups (estimated from reactor-quoted fluxes) of approximately 1.75 a/o (13,000 MWD/T) and 1.93 a/o (14,300 MWD/T) for the top and bottom specimens, respectively. Capsule BMI-23-5, containing uranium-4.6 w/o carbon specimens, was irradiated in Position A-30-NE for six cycles with uranium burnups (estimated from reactor-quoted fluxes) of about 0.66 a/o (4940 MWD/T) and 0.70 a/o (5270 MWD/T) for the top and bottom specimens, respectively.

The postirradiation examination of the specimens was initiated at the hot cell after they were removed from their respective capsules. These examinations included measurements of dimensions and density, and macro examination of the specimens.

Tables K-1 and K-2 list the preirradiation and postirradiation data obtained from the specimens in Capsules BMI-23-3 and BMI-23-5; and Table K-3 lists the mean core and surface temperatures obtained from thermocouples during irradiation of both capsules.

An examination of the data indicates that the UC behaved very well under the temperatures and burnup conditions which the specimens experienced in both capsules. Relatively small changes in density and diameter were produced in the UC due to irradiation. Macro examination of the specimens revealed evidences of cracking throughout the specimens, although the carbide remained in fairly large pieces. It was not possible to obtain measurements of length on any specimen.

At this time, work is being completed on the microscopic examination of the specimens, and an analysis is being made of the fission gas released by the specimens during irradiation. The results of the metallographic examination and of the fission-gas analysis, plus burnup determinations, should provide a more accurate picture of the results. Due to the difficulty in obtaining valid burnup figures based on radiochemical analyses, it has been decided to send two samples of UC to the Chemical Processing Plant in Idaho for isotopic analysis. Comparison of the isotopic analysis, the results of a dosimetry analysis for burnup, and the radiochemical burnup determination should aid in clarifying the situation as far as burnup is concerned.

TABLE K-1. PREIRRADIATION AND POSTIRRADIATION DENSITY MEASUREMENTS OF UC SPECIMENS IN CAPSULES BMI-23-3 AND BMI-23-5

Capsule	Specimen	Density		
		Preirradiation, g per cm^3	Postirradiation, g per cm^3	Change, per cent
BMI-23-3	AI-28 (top)	13.451	13.200	1.8
	AI-29 (bottom)	13.458	13.211	1.8
BMI-23-5	AI-42 (top)	13.744	13.410	2.4
	AI-50B (bottom)	13.327	13.600	1.6

TABLE K-2. PREIRRADIATION AND POSTIRRADIATION DIAMETER MEASUREMENTS OF UC SPECIMENS IN CAPSULES BMI-23-3 AND BMI-23-5

Capsule	Specimen	Diameter				
		Preirradiation, in.	Postirradiation[a], in.			Change[b], per cent
			Point 1	Point 2	Point 3	
BMI-23-3	AI-28 (top)	0.3748	Due to condition of specimen, diameter measurements could not be taken			
	AI-29 (bottom)	Two pieces were measured from this specimen				
	Piece 1	0.3755 Initial value	0.3792	0.3790	0.3780	0.8
		Rotated 90 deg	0.3794	0.3790	0.3766	
	Piece 2	0.3755 Initial value	0.3789	0.3795	0.3792	0.9
		Rotated 90 deg	0.3790	0.3791	0.3784	
BMI-23-5	AI-42 (top)	0.3744 Initial value	0.3781	0.3775	--	0.8
		Rotated 90 deg	0.3776	0.3768	--	
	AI-50B (bottom)	Two pieces were measured from this specimen				
	Piece 1	0.3759 Initial value	0.3812	--	--	1.5
		Rotated 90 deg	0.3820	--	--	
	Piece 2	0.3759 Initial value	0.3800	0.3800	--	0.95
		Rotated 90 deg	0.3790	0.3791	--	

(a) Specimens were measured at three points (where possible) and then were rotated 90 deg for three additional readings.
(b) Change based on average of all preirradiation measurements.

TABLE K-3. MEAN AND MAXIMUM SURFACE AND CORE TEMPERATURES OF SPECIMENS FROM CAPSULES BMI-23-3 AND BMI-23-5

Capsule	Specimen	Surface Temperature, F		Core Temperature, F	
		Maximum	Mean	Maximum	Mean
BMI-23-3	AI-28 (top)	890	765	1550	1178
	AI-29 (bottom)	710	623	1640(a)	1086(a)
BMI-23-5	AI-42 (top)	990	882	1420	1326
	AI-50B (bottom)	850	772	1440(a)	1248(a)

(a) Estimated.

Preparation of UC Pins for Irradiation in the SRE

C. K. Franklin, W. J. Hildebrand, E. L. Foster, and R. F. Dickerson

Appreciable quantities of cast UC are being prepared to evaluate the performance of UC in the SRE at elevated temperatures. Since the surface condition of this material is of interest in the irradiation program, specimens having both as-cast and machined surfaces are being considered.

Approximately 90 in. of cast specimens 0.610 ± 0.002 in. in diameter has been produced by the drop-casting technique. Half of this material was surface ground, providing equal amounts of material showing each type of surfaces.

Various tests were performed to determine the preirradiation qualities of the cast material. Densities of the finished specimens were found to be 98 to 99 per cent of the theoretical value. Electrical-resistivity measurements, obtained along the lengths of the specimens, ranged from 24 to 54 microhm-cm. To establish the internal soundness of the cast specimens, radiographic examinations were made. Results of this test showed the material to be uniform. Only small, isolated voids were detected along the vertical center line of some specimens.

Chemical analyses and metallographic examinations were also conducted. Compositions of the finished specimens varied from 4.85 to 5.15 w/o carbon. Metallographic examinations also showed the carbon content to be in excess of the stoichiometric composition. Thin platelets of UC_2 were observed within the grains in a Widmanstätten pattern and, to some extent, along the grain boundaries.

The preparation and preirradiation evaluations of all UC specimens has been completed, and no further work is planned.

L-1

L. TANTALUM AND TANTALUM ALLOYS

J. H. Stang

Research for Los Alamos Scientific Laboratory (LAMPRE program) is reported in this section. Presently included in the program are two investigations that have been in force for several months. These are (1) a study to develop binary tantalum alloys for the containment of molten plutonium-alloy fuels and (2) a study of the effect of irradiation on the mechanical properties of tantalum. In the former program, a new group of elements has been selected for addition to tantalum; as in the past, alloys will be arc melted, processed to strip, subjected to certain metallurgical screening tests, and forwarded to LASL for plutonium-alloy compatibility studies. In the latter program, two MTR capsule irradiations involving tensile specimens of tantalum have been completed, and preparations are now being made at the Battelle Hot-Cell Facility for postirradiation evaluations.

During November, another investigation involving tantalum was initiated. Phase-identification studies are involved as are studies of the solid solubility of interstitial impurities over a wide temperature range. These studies have resulted from the fact that grain-boundary contaminants are known to have an adverse effect on the corrosion resistance of tantalum in molten-plutonium fuel mixtures. These phases are present even in very pure metal, indicating that the solid solubility limits are exceeded. It is hoped that the identification of these phases can suggest which might be linked with corrosion behavior. Once identified, it might be possible to develop metallurgical practices directed specifically toward their elimination.

Development of Container Materials for LAMPRE Applications

D. C. Drennen, M. E. Langston, C. J. Slunder, and J. G. Dunleavy

Preparations are being made for the arc melting of a large number of binary tantalum alloys for Los Alamos tilting-furnace molten-plutonium corrosion screening. The elements to be investigated in this group are aluminum, beryllium, boron, cerium, hafnium, iron, lanthanum, scandium, silicon, thorium, titanium, uranium, yttrium, and zirconium. The additions of these elements to tantalum will range from 0.5 to 3.0 w/o. The alloys will be arc melted and processed to annealed strip in two groups; those elements of greater interest, such as hafnium and zirconium, will be included in the first group.

Effect of Irradiation Damage of Tantalum

C. K. Franklin, F. R. Shober, and R. F. Dickerson

This study is concerned with obtaining information about the mechanical properties of irradiated and comparable unirradiated tantalum in an attempt to establish the

effect of the transmutation of tantalum to tungsten during irradiation on strength and ductility. Two capsules, each containing six tensile specimens of tantalum, were irradiated at the MTR. The capsules were designed to maintain the specimens at a temperature below 250 F during the irradiation. Capsule BMI-25-1 was irradiated to approximately 7×10^{20} nvt (thermal flux); it is estimated that this dosage resulted in a tantalum-to-tungsten conversion of approximately 1-1/2 w/o. Capsule BMI-25-1 was irradiated to approximately 1.4×10^{21} nvt; the conversion was estimated at approximately 3 w/o. Nickel-cobalt and pure nickel wires were inserted into the capsules for determination of thermal and fast flux, respectively.

Irradiation of these capsules was completed during October, and they were returned to the Battelle Hot-Cell Facility for opening. The specimens have been recovered, and plans are completed for postirradiation mechanical-property tests. These tests will include hardness determinations and tensile-strength and ductility measurements.

Parallel tests will also be conducted on tensile specimens of arc-melted tantalum-1.5 and -3 w/o tungsten alloy. The specimens required have been machined and annealed. The tantalum-1.5 w/o tungsten alloy was annealed at 1150 C for 45 min, while the higher alloy was annealed at 1400 C for 1 hr. These annealing temperatures and times produced a completely recrystallized structure similar to that of unalloyed tantalum.

Precipitate Phase Identification and Interstitial-Type Solid Solubility in Tantalum

D. A. Vaughan and C. M. Schwartz

To aid in the development of container materials for molten-plutonium fuel mixtures, a program has been initiated to identify the precipitate phases in commercial tantalum and to determine the composition and distribution of the initial precipitates caused by interstitial (carbon, nitrogen, and oxygen) impurities. Estimates will be obtained for the solid-solubility limits of these impurities in tantalum at 500, 1000, and 1500 C.

Preliminary studies have been made with three sources of tantalum: (1) Temescal metal electron-beam melted, (2) Temescal metal arc melted at Battelle, and (3) Fansteel arc-cast metal. Electron-metallography and X-ray diffraction examinations of these three materials revealed marked differences which have been ascribed to both interstitial- and substitutional-type impurities. After annealing at 2600 F, very small amounts of precipitate phase or phases were detected in the Temescal metal. Considerable precipitate phase was observed, however, in the Fansteel tantalum. This precipitate phase is believed to be due to the higher oxygen and nitrogen content of this material, since X-ray diffraction studies showed a significant increase in the unit-cell dimensions of the Fansteel tantalum (from 3.3030 A to 3.3037 A). The presence of the precipitate phase would indicate that the solid solubility at 2600 F for either nitrogen, oxygen, or the combination in tantalum was exceeded. Conversely, the unit-cell

dimension of Battelle arc-melted Temescal tantalum was significantly lower (3.3016 A) than that of the electron-beam-melted tantalum. This has been tentatively attributed to tungsten pickup during arc melting. The absence of precipitates in these materials indicates that the tungsten picked up is completely soluble in the tantalum in the annealed condition.

A selection of high-purity tantalum is being made for the interstitial-type solid-solubility studies. For this investigation, it is planned to use one heat of pedigree tantalum with particular attention being placed on the tungsten content. High-purity tantalum from National Research Corporation is being evaluated for this investigation. Nitrogen and oxygen will be added by gas-solid reaction. The specimens will be homogenized and quench annealed prior to electron-metallographic and X-ray diffraction examinations.

DECLASSIFIED

M-1 and M-2

M. DEVELOPMENTAL STUDIES FOR THE PWR

R. W. Dayton

Studies have been begun on the preparation of large fuel plates containing UO_2 platelets. The initial results have been satisfactory.

Fabrication of Large-Scale PWR-Type Fuel Plates

S. J. Paprocki, E. S. Hodge, and C. S. Simons

The feasibility of preparing small-scale Zircaloy-clad uranium dioxide compartmented fuel plates has been established. Process-development studies are now being conducted to assist Bettis in establishing production procedures for the PWR-type Core 2 elements by gas-pressure bonding.

The present program is intended to determine the feasibility of pressure bonding large-size Zircaloy-2-clad UO_2 plate-type fuel elements. An objective of this study is the simplification of the present cleaning and assembly cycle to facilitate production applications.

The components for three prototype PWR elements measuring 33.860 by 4.125 by 0.151 in. and containing 220 core platelets, eleven cores wide by twenty cores long and four 40 by 4.218 by 0.150-in. fuel plates containing 330 core platelets, eleven compartments wide by six compartments long with five cores per compartment, have been received for assembly, bonding, and evaluation. The three 33.860-in. pieced-component fuel plates have been washed, assembled, bonded, and are presently being evaluated. One of the specimens was sectioned longitudinally with one half being sent to Bettis for examination, and the other half being sectioned further for evaluation at Battelle. Sections are being subjected to corrosion testing, burst testing, and metallographic examination.

The initial burst testing of this specimen, in the as-bonded condition, has been completed. Normal bursts occurred in all cases at an average pressure of 3100 psi and an average cladding deflection of 20 mils. This testing also revealed that there is no intercompartmental leakage in this bonded specimen. The corrosion testing and metallographic examination have not been completed.

The four 40-in. specimens have been washed and assembled and are presently in the process of being bonded. In these specimens the core platelets are placed in 100-mil-deep recessed compartments machined into a Zircaloy-2 plate approximately 125 mils thick. Addition of a top cover plate completes the assembly of the component for bonding.

Variations of the present cleaning cycle will be tried in future testing in an effort to determine the minimum preparation necessary for obtaining satisfactory metallurgically bonded fuel plates.

N-1

N. DEVELOPMENTS FOR THE MGCR

W. C. Riley

Research on core materials in support of the MGCR program is in progress at Battelle. The major effort is on the development and evaluation of UO_2 dispersions in BeO or Al_2O_3 and dispersions of UC and UC_2 in graphite. Currently, the evaluation consists mainly of static-capsule irradiation in the MTR and in the BRR.

A study of diffusion of fission products through fuel-element cladding materials is in progress.

FABRICATION AND CHARACTERIZATION OF FUEL MATERIALS

A. B. Tripler, Jr.

Work on fabrication and characterization of fuel materials was recessed during November.

HIGH-BURNUP IRRADIATION EFFECTS IN FUEL MATERIALS

W. E. Murr, N. E. Miller, J. E. Gates, and R. F. Dickerson

A study of the radiation stability of ceramic-type fuels at a specimen-surface temperature of about 1500 F is in progress. The study includes the irradiation, examination, and evaluation of four types of fuel materials: one consisting of about 20 volume per cent uranium dioxide in beryllium oxide (UO_2-BeO), another containing about 20 volume per cent uranium monocarbide in graphite (UC-graphite), a third containing about 20 volme per cent uranium dicarbide in graphite (UC_2-graphite), and a fourth containing about 20 volume per cent UO_2 in Al_2O_3 (UO_2-Al_2O_3).

Three instrumented capsules, each containing two specimens of each of the first three fuel types mentioned above, have been in operation at the MTR since the beginning of Cycle 125 (July 24). The capsules are currently operating in Cycle 130 which is scheduled to terminate on November 23, 1959. A summary of the temperature and heater-power consumption of the three capsules obtained near the beginning of Cycle 130 is shown in Table N-1. A comparison of the heater-power requirements in Cycle 130 with those in Cycle 129 shows that during Cycle 130 Capsule BMI-31-1 required a slightly higher electrical input, Capsule BMI-31-2 remained unchanged in power adjustment, and Capsule BMI-31-3 required less electrical power to maintain the specimens at the 1500 F temperature level. At the present time, all three electrical heaters and four of the six thermocouples in each capsule are operating satisfactorily.

TABLE N-1. TEMPERATURE AND ELECTRICAL-HEATER-POWER CONSUMPTION FOR CAPSULES BMI-31-1, BMI-31-2, BMI-31-3, DURING MTR CYCLE 130

Capsule	Electrical-Heater-Power Consumption	Thermocouple Reading[a], F					
		Thermocouple 1	Thermocouple 2	Thermocouple 3	Thermocouple 4	Thermocouple 5	Thermocouple 6
BMI-31-1	800	--	1500	1475	1460	1280	--
BMI-31-2	2220	1390	--	1420	--	1495	1455
BMI-31-3	2160	1415	1495	--	1455	--	1440

(a) Specimen-surface temperatures are calculated to be 25 to 30 F higher.

A calculation of the burnup incurred in the specimens based on thermocouple readings and heater-power inputs is being made. This calculated burnup value will serve as a basis for determining the number of reactor cycles to which the three capsules will be subjected.

A capsule containing Al_2O_3-UO_2 fuel material is being irradiated in the BRR. The capsule was designed and built by a cooperating laboratory. Battelle has assumed the responsibility of final capsule assembly, hazard evaluation, and conduction of the irradiation experiment. During the first cycle (2 weeks), the peak fuel-cladding temperature was about 1500 F. The peak temperature was increased to 1600 F at the beginning of the second cycle. After 3 days at this temperature, the capsule heater failed. Currently, the average peak fuel-cladding temperature is approximately 1450 F. It has been requested by the cooperating laboratory that this irradiation be extended to a total of six cycles, which will be completed December 28, 1959.

DIFFUSION OF FISSION PRODUCTS IN CLADDING MATERIALS

S. G. Epstein, A. A. Bauer, and R. F. Dickerson

The diffusion of fission products in "A" Nickel cladding is being investigated. Introduction of fission products in the "A" Nickel was accomplished by irradiation recoil from enriched uranium mechanically bonded to "A" Nickel foils.

It was planned to qualitatively analyze for cerium in layers etched from the "A" Nickel foils by radiochemical techniques. However, these techniques are still in the developmental stage, and meaningful results could not be obtained. Work on this project has been recessed.

CARBON-TRANSPORT CORROSION STUDIES

N. E. Miller, D. J. Hamman, J. E. Gates, and W. S. Diethorn

Selected metal and graphite specimens have been exposed to radiation in helium-filled quartz tori designed to promote convective flow of the helium and gaseous impurities past the specimens. The initial results were reported in BMI-1366. Additional metallography and microhardness tests are under way.

P-1

P. DEVELOPMENTAL STUDIES FOR THE SM-2

S. J. Paprocki

Studies are being conducted in assistance to Alco Products that are concerned with the development of fuel, absorber, and suppressor materials for the SM-2.

Full-size reference stainless steel-UO_2 fuel plates containing ZrB_2 burnable poison have been fabricated for critical-assembly tests being conducted by Alco. Additional elements are being evaluated at Battelle to determine structure, bond integrity, and boron and uranium content, and to establish dimensional specifications. Analyses indicate no loss of boron during vacuum sintering of fuel cores; however, an average boron loss of about 7 per cent occurs during roll fabrication. This loss can be controlled to achieve the specified ±5 per cent boron content by use of an initial 5 per cent overload of boron. An evaluation of chromium-, niobium-, and tungsten-coated ZrB_2 is also planned to determine if the boron loss occurring during rolling can be further decreased or completely eliminated.

Reference and modified subsize fuel specimens are being irradiated in three noninstrumented capsules in the MTR and one instrumented capsule in the ETR. It is planned to fabricate and irradiate six additional instrumented capsules in the ETR.

Materials Development

S. J. Paprocki, D. L. Keller, G. W. Cunningham, A. K. Foulds, D. E. Lozier, and W. M. Pardue

Reference fuel suppressor and absorber materials have been selected for the SM-2 reactor. Techniques are being developed for fabrication of these materials into fuel and absorber plates.

Fuel Materials

The reference fuel plate contains a core of approximately 26 w/o UO_2 and 1 w/o natural ZrB_2 dispersed in a Type 347 prealloyed stainless powder matrix (0.030 in. thick) and clad with 0.005-in.-thick Type 347 stainless steel. Major emphasis is being placed upon the production of full-size fuel elements for use by Alco Products in critical-assembly tests and welding studies. Small-scale specimens are also being prepared for use in evaluation of fabrication techniques.

Twenty-eight fully enriched SM-2 fuel plates have been fabricated for critical-assembly tests, and twenty of these plates have been shipped to Alco. The remaining eight plates are being used for metallographic examination and uranium and boron analyses.

P-2

Surface defects were observed in some of the flat annealed specimens. The specimen surfaces were marred with pinpoint spots surrounded with a halo effect after flat annealing. A section of fuel plate containing one of these spots has been removed and is being examined metallographically. The plates which spotted were spray coated with MgO before flat annealing to prevent sticking. It is suspected that some impurity in the MgO caused the spotting, and high-purity alumina has been used on the remaining plates. The last plates exhibited no spots after flat annealing.

As a check on boron losses during sintering, small 1 by 1-in. compacts were sintered along with the enriched cores. One of these cores was then roll clad using the same procedures used for the full-size fuel plates. All of these specimens were then analyzed for boron content. In addition, sections from two full-size depleted UO_2 fuel plates were analyzed for boron content. The results and computed losses are listed in Table P-1. Additional specimens obtained from rejected plates are also being analyzed for boron content.

As previously discussed, these results clearly demonstrate that boron losses can be effectively prevented during sintering by sintering in vacuo. It should be noted that each specimen was obtained from a separate sintering run.

TABLE P-1. EFFECT OF SINTERING ON BORON CONTENT

Sample	Boron Content[a] As Pressed, g	Boron Content[b] As Sintered, g	Change in Boron Content, per cent
DAR-60	0.0521	0.0538	+3.27
DAR-61	0.0521	0.05099	-2.13
DAR-62	0.0521	0.05153	-1.09
DAR-63	0.0521	0.05184	-0.50
DAR-64	0.0521	0.05189	-0.40

(a) Based on weight of ZrB_2 added and previous analysis of boron in ZrB_2.
(b) Sintered 2 hr at 2150 F in vacuo.

The effect of roll cladding on boron loss has not been clearly established. The boron content of the cladding of a specimen which was reported to have an 8 per cent boron loss during fabrication was found to be 0.002 w/o. This amount of boron is considerably lower than the solubility limit of approximately 0.10 w/o boron in gamma iron and thus cannot be readily detected by metallographic means. However, it is not believed to be so low as to preclude loss of boron by diffusion and reaction with oxygen at the surface. Additional studies are in progress to clarify this point. Estimates of boron loss based on chemical analyses of specimens obtained from two full-size plates as well as one value obtained by analyzing an entire small-scale clad core are shown in Table P-2. These losses are well within the range where it should be possible to accurately control the boron loss by proper control of fabricating conditions. A series of specimens recently fabricated should provide additional information on the effect of varying roll-cladding conditions.

Control of boron loss may also be possible through the use of metal-coated ZrB_2 particles. Niobium-coated ZrB_2 has been prepared by vapor deposition in a fluidized bed and will be used in these studies. Metallographic examination of the particles shows a uniform 5-μ niobium coating and no indication of reaction. Coatings of chromium and tungsten will also be evaluated.

TABLE P-2. BORON LOSSES DUE TO ROLL CLADDING

Specimen	Boron Content As Pressed, g	Boron Content As Roll Clad, g	Boron Loss, per cent
DAR-59[a]	0.0521	0.0475	8.85
AR-44[b]	--	--	8.96
DAR-56A	0.0542[c]	0.0524	3.33
DAR-56B	0.0547[c]	0.0499	8.77
DAR-56C	0.0534[c]	0.0501	6.19

(a) Small-scale specimen; entire specimen analyzed.
(b) Exact area of analyzed coupon not known; loss estimated on the basis of three samples.
(c) Boron content estimated as fraction of total core content.

Development of Control and Suppressor Materials

Studies are presently being made to evaluate the use of a Type 347 stainless steel-Eu_2O_3 dispersion for use as an absorber material. An initial corrosion test was conducted at Alco Products on dispersion specimens containing 33 w/o Eu_2O_3 prepared at Battelle. The Eu_2O_3 particles used in these specimens were prepared by the KAPL method of sizing particles before sintering. The specimens in this test failed by severe swelling within a 24-hr test period. There is some evidence that the Eu_2O_3 may have been contaminated during sintering. A sample is being analyzed, but results are not available. Additional specimens are now being prepared by this and other techniques for corrosion testing.

One type of Eu_2O_3 being considered was obtained from a commercial source. This material has been examined petrographically, spectrographically, and by X-ray diffraction and found to have a monoclinic crystal structure. Each crystal is completely fused, leaving smooth crystal planes and a volume porosity of 0.1 per cent. The spectrographic analysis reports the presence of the following impurities in their oxide form:

Element	Amount, w/o
Aluminum	0.05
Calcium	0.03
Cerium	<0.005
Gadolinium	<0.005
Iron	0.01
Lanthanum	0.03
Magnesium	0.01
Silicon	0.01
Thorium	<0.01

Dispersions containing 33 w/o of this Eu_2O_3 are being prepared and roll clad with Type 347 stainless steel and a low-silicon-content stainless steel barrier foil.

Another type of Eu_2O_3 is being prepared by the ORNL process. Several batches of Eu_2O_3 have been pressed in a die at a 4-tsi pressure and sintered for 3 hr at 3090 F in both reducing and oxidizing atmospheres. It was observed that during sintering the material was contaminated with silicon from the furnace muffle. Changes of the furnace muffle are being made to correct this difficulty.

Encapsulation Studies

A. K. Hopkins, W. E. Murr, and J. H. Stang

Reference fuel-plate specimens containing cores of 26 w/o UO_2 and 1 w/o natural ZrB_2 and modified fuel materials containing varying amounts of boron and up to 40 w/o UO_2 are being tested under irradiation. Three noninstrumented capsules are being irradiated in a core position in the MTR. One instrumental capsule is being irradiated in the ETR. It is planned to fabricate and irradiate six additional capsules in the ETR. The capsules have been designed to achieve a specimen-surface temperature of 600 F with a fission heat-release rate at the initiation of irradiation of over 1×10^6 Btu per hr per ft^2 of specimen surface. Target burnups range from 37 to over 70 per cent of the uranium-235 atoms present.

As reported in BMI-1391, the three MTR capsules (BMI-32-1, BMI-32-2, and BMI-32-3) were removed from the reactor during Cycle 129 because they were suspected of contributing to a release of activity into the reactor process water and exhaust gases. After numerous inspections, BMI-32-1 and BMI-32-2 were returned to their original core positions (L-53 and L-56, respectively) for Cycle 130 (starting November 11). At the start of Cycle 131, BMI-32-3 was returned to Position L-58. It is expected that the irradiations will continue in a normal fashion.

During ETR Cycles 22 and 23, thermocouple data from Capsule BMI-32-4 indicated that specimen temperatures were being maintained in the 600 to 650 F range. Since the auxiliary electrical heaters in this capsule have failed, this temperature cannot be regulated and can be expected to decrease as the irradiation progresses and fissionable material is spent.

The construction of another capsule, BMI-32-5, for irradiation at the ETR is well under way. As in the case of BMI-32-4, this capsule will be equipped with six 2-kw auxiliary electrical heaters and four specimen-temperature-monitoring thermocouples. The only major alteration in the design will be to the sheathed heater-to-leadout wire connector system. Laboratory tests of various connector schemes are currently under way to evaluate their general utility and reliability. One phase of this testing program involves an examination of the effect of sustained temperature on the dielectric characteristics of the inorganic potting material employed in the connector system of BMI-32-4. After several hundred hours at 500 F, there has been no evidence

of dielectric breakdown of this material. Since it is suspected that an insulation breakdown contributed to the heater failure in BMI-32-4, there is good reason to believe that an irradiation-damage effect was involved in the capsule-heater failure.

Capsule BMI-32-5 is scheduled to be completed before the end of December. Before shipment to the ETR, however, its heater and thermocouple system will be subjected to a variety of rigorous integrity checks.

Q-1

Q. GAS-COOLED REACTOR PROGRAM

D. L. Keller

Studies for Aerojet-General Nucleonics (AGN) directed toward the development of compact gas-cooled reactors are reported in this section. The activities on the various tasks are reported under "Materials Development Program" and "In-Pile-Loop Program".

MATERIALS DEVELOPMENT PROGRAM

D. L. Keller

In the re-evaluation of the performance of the UO_2 specimens contained in Capsules BMI-27-1 and BMI-27-2, major attention has been given to examining the variation of fission heat along the length of the fuel specimen. An analog experiment has indicated that gradients as large as 250 F might have been sustained along the cladding adjacent to the UO_2 core.

One UO_2 specimen in Capsule BMI-27-2 was punctured and 6.2 per cent of the gaseous fission products formed during irradiation were released. No central melting or sintering was observed in this specimen.

Visual examination of the metal-clad graphite-UO_2 specimens in Capsule BMI-29-1 showed little or no effects of irradiation. Measurements indicated virtually no changes in the exterior dimensions or the over-all specimen densities.

Hot-cell evaluation of the 19-pin in-pile-loop assembly, IB-1βT, is under way.

Experiments with the ML-I-1A critical assembly were completed during the past month. Final experiments were concerned with studying the reactivity worth, powder distribution, and flux distribution of a mock-up of the 19-pin fuel assembly at various positions in the critical-assembly core.

Fabrication of BeO-UO_2 Fuel Pellets

H. D. Sheets and C. Hyde

Pellets of UO_2-containing BeO ceramic are being prepared for irradiation in both loop and capsule exposures.

Current effort is directed toward fabricating pellets for capsule irradiation in the BRR. At the same time, necessary process development in anticipation of fabricating about 2500 pellets for a loop-irradiation experiment is being done.

Q-2

Encapsulation Studies

J. H. Stang, J. F. Lagedrost, G. E. Raines, and
D. W. Nicholson

Irradiation of Clad Pin-Type Specimen Containing Dense UO_2

As a part of the postirradiation-examination phase of specimens irradiated in Capsules BMI-27-1 and BMI-27-2, the capsule thermal performance is being re-evaluated in some detail. As indicated in previous reports, several of the specimens in these capsules failed during the irradiation in a manner that would suggest overheating effects. However, readings from thermocouples located adjacent to the specimens indicate that the cladding temperatures did not exceed 1800 F for any significant period of time.

Inconel-clad (30-mil cladding) UO_2-containing (35 per cent enriched) specimens, 0.225 in. in OD, were irradiated in these capsules. In one type, the UO_2 was present as a stack of six 0.167-in.-thick pellets; in another type the UO_2 had the form of a 1-in.-long cylindrical shell (e.g., an SIR pin design). In appraising factors which might contribute to specimen failure, major attention has been devoted to exploring the possibility that cladding hot spots occurred as a result of higher-than-average heat-release rates at the ends of the fueled regions where self-shielding effects were minimum. According to estimates of the variation of fission heat with axial position, based on simplifying assumptions, the end pellets in the stacked-pellet specimen design could have generated approximately 30 per cent more heat than the central pellets. Also, it would appear that the very ends of these end pellets could have generated over 60 per cent more heat than the central pellets.

To appraise the effect of high local heat-release rates on specimen temperature, a geometrical-electrical-analog experiment, employing Telledeltos paper as the conducting medium, was conducted during November. Axial sections of the specimen and NaK regions were simulated with an isothermal boundary assumed at the edge of the NaK; variations in heat generation with position along the specimen axis were simulated by appropriate current sources. While this model was not exact because of the inability to compensate for radial heat-flow effects at the reference plane chosen, it demonstrated that gradients as large as 250 F might be sustained along the cladding assuming a typical in-pile heat-release rate and the axial heat-generation variations suggested above. The corresponding top clad section-to-thermocouple (located adjacent to the central pellets) gradient was approximately 350 F.

According to these results, a temperature of 1700 F sensed by a thermocouple could reflect a peak cladding temperature of 2050 F. While this is somewhat below the melting point of Inconel, fairly low stresses might cause a cladding failure at such a temperature. Stress calculations are being made to evaluate this possibility. Heat-transfer analyses are also being continued in an attempt to reduce the uncertainties now existing.

Irradiation of Specimens Containing MCW Spherical UO_2 Dispersed in Stainless Steel

Capsule BMI-33-1 was inserted in the MTR at the beginning of Cycle 131 (starting on November 25); Capsule BMI-33-2 probably will be inserted at the beginning of Cycle 132. These capsules each contain clad specimens fueled with 30 w/o UO_2 dispersed in stainless steel; two types of UO_2, MCW spherical and ORNL hydrothermal, are involved and will be compared as regards irradiation stability.

The first capsule inserted is scheduled for a three-cycle irradiation to achieve a fission burnup of approximately 9 per cent. The latter will be irradiated for two reactor cycles. In each case, the design specimen-core temperature is 1650 F.

Irradiation of UO_2-Graphite Specimens With an Integral Corrosion-Gas-Flow System

As indicated in BMI-1391, this irradiation-capsule program has been curtailed, the present objective being only the completion of the capsule design and the hazards analysis. These phases of the program, which are requiring a minor effort, continued during November and will be completed by the end of December.

Irradiation of Specimens Containing UO_2 Dispersed in BeO

This experiment is designed to investigate the irradiation stability of Hastelloy X-clad dispersions of UO_2 in BeO at 1725 F. A total of six specimens will be contained in a 1-1/8-in.-OD double-wall stainless steel fully instrumented capsule and irradiated at the BRR in an unperturbed thermal flux of 4.2×10^{13} nv. Each specimen consists of five 0.160-in.-diameter pellets; the three central pellets are 1/4 in. long and contain 25 volume per cent UO_2, the two 1/8-in.-long end pellets contain 17 volume per cent UO_2. This loading arrangement was devised to reduce the possibility of local overheating caused by higher-than-average rates of fission-heat generation by the end pellets.

Nuclear-mock-up tests, in which the specimens were simulated by cobalt pins, were run in BRR Position 12 during October, and unperturbed-flux values were determined for BRR Positions 12 and 45 during November. Final results of dosimeter analyses from these tests indicate that:

(1) The peak unperturbed flux in each position is approximately 4.2×10^{13} nv.

(2) The average effective flux within the three central pellets of the peak-flux specimen can be expected to be 1.3×10^{13} nv; the corresponding flux within the 1/8-in. end pellets is 1.5×10^{13} nv. Thus, since compensated fuel loading is being employed, an acceptable heat-generation profile along the specimen axis can be expected.

Q-4

The capsule design, fabrication, and operational-analysis details are being completed so that irradiation can begin shortly after the specimens become available, probably about January 1.

Effects of Irradiation

J. H. Saling, J. E. Gates, W. E. Murr, and R. F. Dickerson

A study of the radiation stability of fuel-element materials for compact gas-cooled reactors includes (1) the evaluation of encapsulated solid and annularly loaded UO_2 specimens clad with Inconel, (2) the evaluation of encapsulated specimens of UO_2 dispersed in graphite and clad with Inconel 702, Hastelloy X, or Carpenter 20 Cb, and (3) the evaluation of in-pile-loop subassemblies containing PWR-type fuel pins of solid UO_2 clad with Inconel.

Capsule Program

Fission-gas release data from Specimen GE-Solid-II, which was the fourth specimen from the top in Capsule BMI-11-7, indicated that 6.2 per cent of the gaseous fission products formed during irradiation were released from the fuel. These calculations were based on an assumed burnup of 4 per cent of the uranium-235, and will be revised when burnups obtained by isotopic analysis are available. The fission-gas release data from the third specimen from the top, MC-Solid-7, is being rechecked.

Difficulties were encountered in obtaining good chemical-analysis samples of the clad material from specimens irradiated in Capsule BMI-27-1. The cladding on these specimens had apparently melted during irradiation. Fresh samples are presently being prepared and will be analyzed by emission-spectrometer and wet-chemical methods in an attempt to determine why the cladding could have melted at the measured irradiation temperatures.

Transverse sections of the solid UO_2 specimen from this capsule were prepared and examined. A void was observed in the center of the UO_2 which may be indicative of central-core melting or sintering. The UO_2 immediately surrounding the void appeared to have a dendritic structure, whereas the UO_2 at the outer surface of the pellet appeared to have a normal structure. Metallographic examinations of the UO_2 and cladding from three different specimens are being performed. Both the UO_2 and the cladding will be examined in the as-polished and in the etched conditions at magnifications up to 500X.

During November, the postirradiation examination of specimens irradiated in Capsule BMI-29-1 was initiated. This instrumented capsule (three 1-kw electric heaters and six thermocouples) contained six specimens of approximately 8 w/o UO_2 in graphite clad with 0.025-in.-thick Hastelloy X, Carpenter 20 Cb, or Inconel 702 tubing. The fueled-graphite specimens were right cylinders approximately 1.0 in. in diameter, and were coated with a 3 to 5-mil-thick layer of silicon-silicon carbide. The over-all dimensions of the clad fuel pins were about 1-7/16 in. long by 5/16 in. in diameter.

Q-5

The capsule was irradiated in MTR Position A-39-SE (estimated thermal flux of about 1.3×10^{14} nv) for Cycles 126 and 127. Thermocouples submerged in NaK adjacent to the specimens indicated that the specimens operated at surface temperatures between 1600 and 1775 F. The capsule was discharged from the MTR after an estimated uranium burnup of 8 a/o. After irradiation the capsule was opened and the individual specimens were recovered.

Samples of gas from the inner capsule cavity, the NaK-butyl alcohol solution, and dosimeter wires located adjacent to the individual specimens are being analyzed. The density and dimensions of each of the six specimens were measured. Each specimen was visually inspected and photographed with the aid of a stereomacroscope.

Results of the density and dimensional measurements of the six specimens are reported in Table Q-1. Changes in dimensions and density were very small, and were generally within the experimental error. Uneven weld beads on the ends of the specimens resulted in wide variations between successive measurements of length.

TABLE Q-1. PHYSICAL MEASUREMENTS OF SPECIMENS FROM CAPSULE BMI-29-1

		Physical Measurements					
		Preirradiation			Postirradiation		
Specimen	Cladding Material	Length[(a)], in.	Diameter, in.	Density, g per cm^3	Length[(a)], in.	Diameter, in.	Density, g per cm^3
1-I	Inconel 702	1.4705	0.3157	4.57	1.4715	0.3153	4.51
2-I	Inconel 702	1.4990	0.3157	4.45	1.4979	0.3146	4.47
3-C	Carpenter 20 Cb	1.4400	0.3143	4.36	1.4356	0.3141	4.36
8-C	Carpenter 20 Cb	1.4657	0.3144	4.37	1.4650	0.3147	4.36
5-X	Hastelloy X	1.4437	0.3112	4.43	1.4488	0.3121	4.41
6-X	Hastelloy X	1.4393	0.3117	4.42	1.4399	0.3117	4.41

(a) Length measurements were taken on top of weld beads, and, therefore, show considerable variation.

More elaborate tests and examinations are now being planned for the six specimens recovered from Capsule BMI-29-1. These tests will be initiated in the near future.

In-Pile-Loop Subassemblies

Subassembly 1B-1αT. The metallographic examination of sections from Subassembly 1B-1αT is being continued. One longitudinal section from the corroded spacer from Pin 16 and a transverse section from Pin 15 is being examined. Also a sample of the corroded fuel-pin spacer from Pin 16 is being prepared for analysis by emission spectrometer and wet chemistry. The results of these examinations will be reported as soon as they become available.

Q-6

Subassembly 1B-1βT. During November, the postirradiation examination of the 1B-1βT loop subassembly was performed. This loop contained 19 fuel pins arranged concentrically as follows: 12 pins were located in the outer ring, 6 pins were located in the inner ring, and 1 pin was located in the center of the inner ring. The pins contained pellets of enriched UO_2 clad with Inconel 702. The cladding was fabricated with longitudinal fins on the outer surface adjacent to the fuel-bearing portion of the pins. This provided a more efficient heat-transfer surface. Twenty-eight thermocouples were strategically placed throughout the loop to measure inlet- and outlet-gas temperatures, and the temperatures of the inner and outer fuel cladding surfaces. The pins containing internal thermocouples were silver soldered at the point of thermocouple exit from the fuel pins. The thermocouple hot junction was separated from the UO_2 fuel by a zirconia disk in order to prevent occurrence of a metallurgical reaction. The fuel subassembly operated for approximately 35 hr in the recirculating gas loop at the BRR before high fission-gas activity in the loop resulted in termination of the experiment. At this time, the loop was transferred to the BMI Hot-Cell Facility for postirradiation examination. The fuel element was examined visually, and appeared to be in excellent condition with no evidence of distortion or gross corrosion. The pin assembly was leak checked prior to disassembly by immersing it in diphenylphthalate, applying a partial vacuum to the liquid container, and noting the location of persistent bubbles. A leak was detected at the location of the thermocouple exit from Pin 16, and another leak was located in the general area of Pins 2, 3, and 4 in the inner ring. It was not possible to pinpoint the leak in the inner ring more closely because of the tendency of the bubbles to travel along the underside of the pins.

After leak checking, the pins were separated from the spacing spider. The individual pins were examined for bowing by rolling them across a flat surface and noting any separation between the ends and center of the pins and the plate. This method of bowing examination was made necessary because of the finned cladding and the fact that some of the spacers were ground flat over part of their periphery. The maximum separation between the pins and plate, as determined by this method, was about 3/16 to 1/4 in. from an imaginary axis running through the center of the pin. It is believed that the bowing was produced during the disassembly operation when a cutting tool broke.

The pins were examined individually on the stereomacroscope for evidence of corrosion and other surface irregularities. Both pins and spacers were in excellent condition, and showed no evidence of corrosion, swelling or cracking. A slight accumulation of scale was observed in the fluted troughs of several pins, being most prevalent on the gas-exit end of the inner ring of pins. The inner ring included Pins 2 through 7.

A motion-picture record was obtained of the sequence of events occurring during the postirradiation examination of the 1B-1βT fuel element. In addition, still photographs and stereomacrographs of the pins were obtained. This concludes the proposed work on the postirradiation examination of the 1B-1βT fuel element.

Q-7

GCRE Critical-Assembly Experiments

J. W. Ray, W. S. Hogan, D. A. Dingee, and J. W. Chastain

Experiments with the ML-1-1A critical assembly were completed during the past month. The assembly will be modified to conduct experiments on the ML-1-1B reactor concept, which is fueled with UO_2 pins.

These final experiments with the present assembly were conducted to evaluate mock-ups of the 1B pin-type fuel element.

Fuel-Element Description

The mock-up of the pin-type fuel element consisted of 19 Inconel X tubes, 0.164 in. in ID and having a 0.030-in. wall, arranged in a three-ring hexagonal lattice. The pin bundle was inserted into a 1.5-in.-OD by 0.015-in.-wall stainless steel insulation liner and this assembly was, in turn, put into a 1.80-in.-OD by 0.02-in.-wall stainless steel pressure tube. The pins were supported axially on an aluminum tube to center the fuel in the ML-1-1A core.

The pins contained both natural and highly enriched uranium-metal foil 22.75 in. long and 0.10 in. wide. The enriched foil was 0.004 in. thick and the natural foil was either 0.015 or 0.020 in. thick. The number of foils in each fuel pin was selected to simulate the uranium dioxide fuel density and a range of enrichments. Table Q-2 gives the designation, simulated enrichments, and total loading of the pin-type fuel elements.

TABLE Q-2. FUEL LOADINGS OF 1B PIN-TYPE FUEL ELEMENTS IN ML-1-1A CRITICAL ASSEMBLY

Element Designation	Enrichment, per cent		Total Uranium-235 in Element, g
	Inner Seven Pins	Outer Twelve Pins	
1B-1	49.7	24.2	278.0
1B-2	93.0	28.8	640.4
1B-3	74.4	35.3	636.4
1B-4[a]	93.0	93.0	632.3

(a) Differs from 1B-3 in that all natural uranium foil was removed; uranium-235 content is the same.

Reactivity-Worth Studies

The fuel elements were substituted, one at a time, for 1A elements in various core positions in the ML-1-1A configuration shown in Figure Q-1. Two positions in the core were empty during all of the experiments. In the core positions used for the 1B elements the reactivity worth was compared with a specially constructed ML-1-1A cylindrical-plate-type fuel element. The special element had an active fuel length of 22.75 in. (similar to the 1B fuel length, regular critical-assembly elements are 28.00 in. long) and the cadium band simulating burnable poison in the ML-1 element was removed. Table Q-3 gives the results of the reactivity studies.

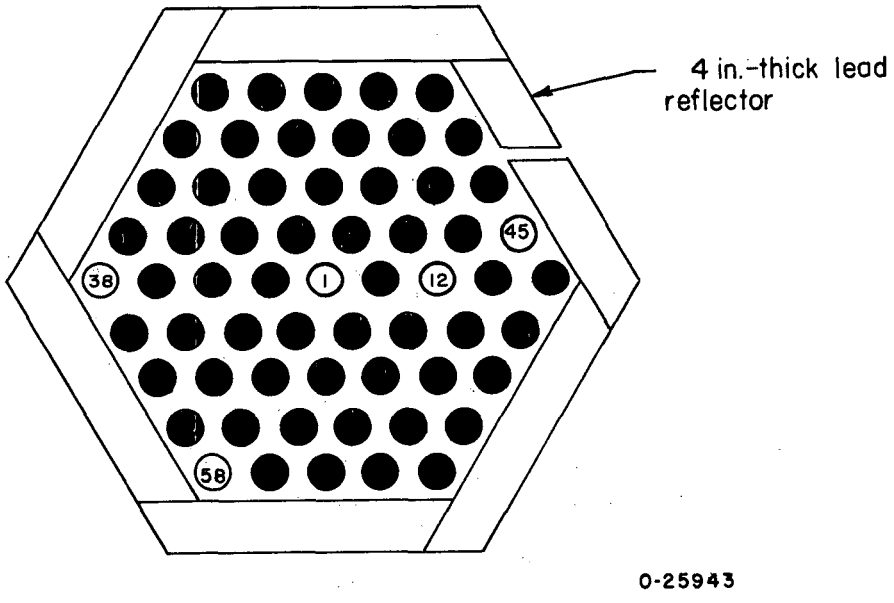

FIGURE Q-1. PLAN VIEW OF ML-1-1A CRITICAL ASSEMBLY SHOWING CORE POSITIONS WHERE 1B PIN-TYPE ELEMENTS WERE TESTED

One 1B element was substituted for one of the 1A elements in Position 1, 12, or 45 in each experiment. Positions 58 and 38 were empty during all of the experiments.

Q-9

TABLE Q-3. REACTIVITY EFFECT OF INTERCHANGING LISTED ELEMENT WITH SHORTENED 1A ELEMENT

Element	Core Position	Reactivity[(a)], Δk/k
1B-1	1	-11.4×10^{-4}
1B-2	1	6.7×10^{-4}
1B-2	12	7.3×10^{-4}
1B-2	45	3.0×10^{-4}
1B-3	12	1.7×10^{-4}
1B-4	1	9.5×10^{-4}
1B-4	12	8.7×10^{-4}
1B-4	45	3.3×10^{-4}

(a) Listed reactivity values are relative to the shortened ML-1-1A element.

Power-Distribution Studies

Power distributions through the pin-type elements were measured at a number of positions in the core by counting gamma radiation from 1/2-in.-long sections of the fuel pin after irradiation. This section was centered 6.875 in. above the fuel midplane. Table Q-4 presents the power-distribution measurements.

TABLE Q-4. DISTRIBUTION OF TOTAL ELEMENT POWER IN 1B FUEL ELEMENT

	Average Power per Pin in 1B Element at Core Position Shown, per cent				
Fuel Element and Position	1B-1, Position 1	1B-2, Position 1	1B-2, Position 12	1B-2, Position 45	1B-3, Position 12
Center pin	5.40	5.18	5.09	5.18	4.49
Pins 2-7 (6 pins second ring)	5.91	6.13	5.90	5.87	5.29
Pins 8-19 (12 pins outer ring)	4.93	4.88	4.94	4.97	5.31

In one case, Element 1B-4, an additional irradiation was performed with a 15-mil cadmium sleeve surrounding the 1/2-in. monitoring section to measure epicadmium power distribution. For pins in the second ring the average cadmium ratio (bare power/cadmium-covered power) was 2.84; in the outer ring this ratio was 4.71.

Flux-Distribution Studies

Thermal flux throughout the fuel element and in the adjacent moderator region was measured using bare and cadmium-covered manganese-copper wires. Table Q-5 summarizes the detailed flux mapping.

TABLE Q-5. THERMAL-NEUTRON-FLUX VARIATION AROUND PIN-TYPE FUEL ELEMENTS

Fuel Element	Core Position	Average Thermal-Neutron Flux at Location Indicated, arbitrary units			
		Moderator	Stainless Steel	Inconel X	Center of Fuel[a]
1B-1	1	3.86	3.06	1.65	(0.85)
1B-2	1	3.87	2.96	1.50	(0.65)
1B-2	12	4.31	3.03	1.59	0.70
1B-2	45	3.43	2.38	1.20	(0.57)
1B-3	12	4.56	3.27	1.64	0.73

(a) Obtained using a manganese-containing wire located at the center of the fuel region. Data were averaged over the quantity of uranium-235 in the various fuel pins. Values shown in parentheses may include a contribution from streaming from the sides, since the measuring wire was located between the two center fuel foils. Other values were obtained with the fuel foils arranged around the wire to decrease streaming.

The studies reported here complete the preliminary evaluation of pin-type elements using the ML-1-1A critical assembly. The critical assembly is being modified to accept uranium dioxide pellet fuel pins to investigate the ML-1-1B core. The loading and enrichment will be similar to the 1B-3 elements described above. During the past month the components of the ML-1-1A critical assembly were dismantled in preparation for the installation of new grid plates, lead reflector, and control blades. These components have been designed and are being fabricated.

It is expected that many of the new components will be available for assembly during the coming month.

IN-PILE-LOOP PROGRAM

G. A. Francis

Battelle is engaged in the design, construction, and operation of in-pile recirculating gas loops for support of the Army gas-cooled reactor program. The two loops are designed for the irradiation of full-size reactor fuel elements at reference conditions.

The loop at the BRR has been used for the evaluation of five fuel specimens and is now being readied for operation of a sixth specimen which will be designed and constructed by AGN. The loop at the ETR has been installed. The blowers or primary-coolant circulators for this loop are at Battelle, where operation and life tests are under way.

Q-11

BRR Loop Program

S. J. Basham and W. H. Goldthwaite

The present preparation for operation is directed toward irradiation of the AGN fuel specimen designated 1B-2T-1, which is scheduled to start during January, 1960. Tasks to be completed before that date include the preparation and approval of an appropriate hazards summary, the performance of a short loop run without a specimen to investigate for the presence of fuel contamination of the loop test section, the replacement of certain process tubing, and the installation of a continuous loop gas-activity monitoring system.

The irradiation of the 1B-2T-1 is scheduled to start in mid-January. In order to maintain this schedule, the hazards summary must be completed during December. The mechanical drawings of the specimen were reviewed during November, and the over-all design will be evaluated when further data and test requirements are received.

A loop run in-pile without a specimen in the test section has been planned to determine the presence of fuel particles in the loop and test section. The run will be of short duration and be performed during December after certain reactor operating problems have been solved.

Prior to the run without a specimen, part of the aluminum process tubing will be changed out and replaced by stainless steel tubing. At the same time, a continuous loop gas-monitoring system will be installed and calibrated. The necessary commercial components have been purchased and should be received early in December. The installation work includes the fabrication and mounting of a stand for the gas monitor, the connection of the detector unit to the count-rate meter and 100-channel analyzer, and the calibration of the entire unit.

ETR Loop Program

E. O. Fromm and J. V. Baum

The BMI-16 loop has been installed at the ETR and the cold check-out has been completed. Difficulty with blower reliability was encountered during the hot check-out, and the four blowers were shipped to Battelle for modification and testing. After the modifications discussed in last month's report (BMI-1391), a blower test was initiated at Battelle. The test was started in October and was terminated after 800 hr of operation at design temperature and flow conditions. The test shows that the modified blowers should operate satisfactorily in the loop application. The blowers meet all of the initial design specifications.

A study of the blower operation at the reactor site and the test data shows that the grease mechanism now installed at the reactor site could be the cause of the temperature excursions which were experienced there. To eliminate the influence of periodic greasing, the test blower was regreased on November 14 and operated until November 27

without additional greasing. On November 27 the blower was stopped and inspected. It was found to be in good operating condition.

The bearing races were examined after the 800-hr run and found to be in excellent condition. Only a small amount of fretting was observed on one bearing. It appears that the additional clearance in the bearing housing has provided expansion space for the bearings and reduced loading due to differential thermal expansion.

The tests demonstrated that a blower can be operated for at least the equivalent of one ETR operating cycle without adding grease to the bearings, and that the operating period can be renewed by the proper regreasing of the bearings. The tests also show that the drive modifications and the modifications of the housing and impeller to eliminate interference and to reduce end thrust have been successful.

During December, it is planned that two modified and tested units will be shipped to the reactor site. Tests will be continued at Battelle on the other two blowers to evaluate a possible new lubricant and to determine the best schedule and mechanism for bearing relubrication. The date of initial specimen irradiation will depend on reactor scheduling, availability of reactor personnel for blower installation, and successful completion of the loop hot check.

RWD:CRT/all